JOURNAL OF THE AERONAUTICAL SCIENCES

VOLUME 9 MARCH, 1942 NUMBER 5

Resin-Bonded Wood Laminates for Shell Type Aircraft Structures

ALFRED A. GASSNER*

Duramold Aircraft Corporation

Introduction

Wood veneers in combination with synthetic resins are now considered as a suitable material for aircraft construction, and one of the first steps of the designer must be to disperse that antagonism or disinterest the average engineer has against wood as such, and against its physical characteristics and properties. Wood as lumber is not homogeneous and it is not isotropic; it is also more sensitive to atmospheric influences than are the metals. Wood veneers plus synthetic resin as bonding medium will react more nearly like a homogeneous material and by suitable design and by consideration of the applied stresses, a construction can be built that will be fully able to carry the required loads, even though the material is not fully isotropic.

Surface coating with synthetic resin finishes makes these structures highly impervious against atmospheric influences and resin impregnation of the basic veneers can be used to make the laminations practically immune against moisture.

These wood-base laminations are exceedingly well suited for the construction of full-stressed shells for aircraft parts with very few internal stiffeners. The design of such shells brings many new problems to the designer, since very little data exist on the allowable stresses for these materials. The behavior of each single lamination of the stressed panel must be considered and studied.

General Remarks on Wood Laminates

One of the laminates developed during recent years is Duramold which is made from wood veneers as base, with phenol-formaldehyde resins of the thermo-setting type as bonding material. Its physical characteristics depend, of course, on those of the basic components and as, in many cases of humanly created products, it is the endeavor of the engineer to improve on nature. It can be safely stated that such wood-plus-resin materials are a better engineering medium than is the original wood. The proper methods of designing and of manufacturing laminated structures from thin layers of wood and the good bonding and high immunity against atmospheric influences derived from the use of the recently developed synthetic resins, gives these structures in comparison to natural wood a status which is somewhat similar to that of metal alloys in parallel to their original metallic components.

Engineers readily admit that a proper mixture of copper and of zinc is better than either of its components; no one wonders any longer when iron is improved by adding very small percentages of other elements; and aluminum, which is a very soft metal, can be toughened by adding small percentages of copper and of zinc.

But the average engineer has little admiration for the oldest building material in the world: wood, and he will not readily admit that wood can be improved.

There are probably only two reasons for the reluctance of engineers to consider natural wood as a first grade technical material—wood is not homogeneous and not isotropic; and secondly, wood is susceptible to atmospheric conditions more readily than are the metals.

Both of these undesirable facts can be eliminated to a very large degree by sensible engineering.

One single piece of wood is not homogeneous and it is not isotropic. Two pieces joined together properly can be made practically isotropic for two directions of loading. But they are not yet homogeneous; each of

Presented at the Structures (Part 2) session, Tenth Annual Meeting, I.Ae.S., New York, January 28, 1942.

* Vice-President—Engineering.

these laminations has still the characteristics produced by nature during the growth of the tree. They may contain fibers from early and from later growth of the tree; they may contain fibers that have grown during spring and during summer, during wet and during dry seasons, which all have a different effect on the structure of the wood.

The first step to create improved wood is therefore the selection of cuts that are to be used of the cross-section of the log. For modern aircraft, the veneers used are either rotary cut, that is, sliced around the circumference of the log, or they are quarter-sliced or wing-beam cut, which are cut radially.

Duramold uses veneers of from $^1/_{48}$ inch to $^1/_{20}$ inch, which are laid up so that grain direction of a part of the layers crosses at right angle to that of the remainder of the layers. The fact that the wood itself is not homogeneous is thereby eliminated to a very large degree, since the adjacent veneers will have different grain figuration. A nearly isotropic material is hereby created; a material that is at least isotropic in some preselected directions. This technique is not new and has been used for years in plywood construction. In manufacturing the usual commercial plywood it is, however, customary to keep the number of laminations for a given panel thickness as low as possible, and to increase the thickness of each lamination. In Duramold design, many very thin veneers are used to obtain the highest possible homogeneity at reasonable cost. While commercial plywood of $^1/_4$ inch thickness is, for instance, built up from five plies, the Duramold construction would use for the same thickness 10 to 12 plies. Commercial plywood is difficult to bend even on large radii, and the bending or forming of commercial plywood to pronounced compound curvature is impractical. Duramold can be molded to small single radii and it can be readily molded to very pronounced compound curved shapes, because each of the very thin veneers is formed separately which requires only small pressures and which introduces hardly any stresses into the single veneer. Then the veneers are formed in the mold to the desired shape, while the layers are bonded together at the same time by the resin. All these phases take place simultaneously.

In airplane design the directions of the stresses are well known for each component part, and the wood laminations can be arranged so that the final material is well able to take care of these stresses.

This should therefore dispose of the first mentioned objection against wood.

The second objection, deterioration under atmospheric conditions, can be overcome by the use of the modern synthetic resins. Deterioration of wood is caused mostly by water and air. Plywoods were, up to a few years ago, glued with blood albumen or with vegetable glues. They could be separated into the original layers when soaked in water. The synthetic resins are absolutely waterproof and the phenol-formaldehyde resins are even proof against boiling water. The inner and outer surfaces of laminated panels are now being treated with paints made from synthetic resins and water is thereby prevented from getting into the wood fibers. A recently developed technique for penetrating all veneers with resins before they are assembled into panels makes the entire structure practically moistureproof so that the wood fibers cannot swell when under high humidity, nor shrink under dry heat.

In these modern wood veneers plus synthetic resin products, we have therefore a material that is as homogeneous and as isotropic as is required and that is protected against deterioration from atmospheric conditions. These basic facts should work to overcome that certain antipathy against wood which came with the modern school of metallurgy, now about 100 years old, that tended to see only metals as full-fledged engineering material. Wood in its modern technical conception should find again a good place in the minds and hearts of engineers. It seemed to be necessary to proceed with this introduction for the sake of eliminating the wrong impressions created by calling these airplane materials "molded plastics." The reaction of the average engineer when told later that these "plastics" could not be poured into a form and that they were not some sort of magic material, but that they had a wood base, resulted in many cases in a somewhat deprecating remark about wood in general.

In this connection it might be well to remember that all-metal airplanes were built for many years with corrugated aluminum alloy sheet as skin material for wings and for fuselages. And corrugated sheet is surely not an isotropic material. Nor is a wing or fuselage skin with its reinforcement stringers, as built today, isotropic. However, in airplane design, the direction of the design stresses is well known and it is almost always possible to arrange the materials so that the line of greatest strength coincides with the line of greatest stress. This principle should therefore tend to eliminate objections against the non-isotropism of wood-base structures.

A desirable material for aircraft construction must have good weight-strength ratio. This does not necessarily mean that a high tensile strength to weight ratio is the most important factor, as will be discussed later on.

Engineers endeavor to create shell type structures which are stable with a minimum of interior reinforcements, and especially free of longitudinal stringers. This can only be achieved if the stiffness of the shell is high, that is, if it has a high value of EI, the product of effective modulus of elasticity, times the moment of inertia of the cross-section. This leads naturally to the selection of wood veneers of low specific gravity and of high values of modulus of elasticity, and to the distribution of the material in the best suited combination of longitudinal and transverse grain veneers. It is

customary to call veneers longitudinal that have grain direction parallel to the major load direction.

Data on Physical Characteristics of Wood Species

Data on physical characteristics of wood species usable for aircraft construction are given by Markwardt.[1] Data on some of the wood species most commonly used are reproduced here in Table 1.

Tensile Strength of Wood

The original report,[1] from which data of Table 1 were taken, states on page 3 that the modulus of rupture in static bending can be used safely for tensile strength parallel to grain.

Trayer[2] gives on page 129, values for tensile strength of a single veneer. These values are calculated from the tensile strength of a three-ply panel, based on the assumptions that the three laminations have the same thickness, that the face plies have grain direction parallel to the applied tension load, and that the core ply, whose grain is perpendicular to the load, carries no load.

However, both methods of calculation do not seem to check when they are applied to data of Table 2-2.[3] In that table, the tensile strength is given for three-ply panels of various species of wood; all plies in one panel have the same thickness and are of the same species, and grain of successive plies is at right angles.

For simple African Mahogany veneers, Trayer,[2] page 129, gives a tensile strength parallel to grain of 8060 lbs. per sq.in. The tensile strength of the three-ply panel parallel to face grain is 5370 lbs. per sq.in., or $^2/_3 \times 8060$ lbs. ANC-5, Table 2-2,[3] gives for tensile strength of a three-ply panel made of African Mahogany, loaded parallel to face grain, a value of 5370 lbs. per sq.in., and for the same panel loaded perpendicular to face grain a value of 3770 lbs. per sq.in. However, by the method suggested by Trayer,[2] the tensile strength perpendicular to face grain should be 8060/3 = 2690 lbs. per sq.in.

Analysis of Three-Ply Panel for Tensile Stresses in the Laminations

It appears that a more exact analysis is required to find the actual stresses for each of the laminations that make up the three-ply panel.

The moduli of elasticity for African Mahogany three-ply panels are given in ANC-5, Table 2-2,[3] for compression loads. They are E_L = 1,261,000 lbs. per sq.in. (for loading parallel to direction of face grain) and E_T = 144,000 lbs. per sq.in. (for loading perpendicular to face grain). From these values of the apparent moduli of elasticity of the panel, the moduli of elasticity of the veneers can be calculated. The moisture content of the test panels had an average value of 12.7 per cent.

It is evident that for a panel under compression loads, the outer laminations contribute more to the stiffness of the panel than do the inner layers.

In the following mathematical discussion constants are defined as follows:

E_L = Modulus of elasticity of three-ply panel when loaded parallel to the direction of face grain.

E_T = Modulus of elasticity of three-ply panel when loaded perpendicular to the direction of face grain.

I = Moment of inertia of three-ply panel about the neutral axis of the cross-section.

E_{fL} = Modulus of elasticity of face veneers parallel to grain.

E_{fT} = Modulus of elasticity of face veneers perpendicular to grain.

E_{cL} = Modulus of elasticity of core veneers parallel to grain.

E_{cT} = Modulus of elasticity of core veneers perpendicular to grain.

I_f = Moment of inertia of face veneers about neutral axis of cross-section of the three-ply panel.

I_c = Moment of inertia of the core veneer about the neutral axis of the cross-section of the three-ply panel.

Table 1

Weight and Strength Values for Various Woods. Based on 15 Per Cent Moisture Content, for Use in Aircraft Constructions

		Static Bending, Lbs per Sq.In.			Compression Maximum Crushing Strength, Lbs. per Sq. In.		
Wood Species	Weight, Lbs. per Cu.Ft.	Fiber Stress at Elastic Limit	Modulus of Rupture	Modulus of Elasticity, 1/1000	Parallel to Grain	Perpendicular to Grain	Shearing Strength Parallel to Grain, Lbs. per Sq.In.
Birch	44	9500	15,500	1780	7300	1590	1300
Afr. Mahog.	32	7900	10,800	1280	5700	1400	980
Honduras Mahog.	34	8800	11,600	1260	6500	1760	860
Poplar, Yellow	28	6000	9,100	1300	5000	810	800
Basswood	26	5600	8,600	1250	4500	620	720
Spruce	27	6200	9,400	1300	5000	840	750

f = Thickness of face veneers (two).
c = Thickness of core veneer (one).
t = Thickness of three-ply panel ($t = f + c$).

The stiffnesses $E_L I$ and $E_T I$ of the three-ply panel are the respective sums of the stiffness of the individual veneers. Parallel to applied load, that is for $E_L I$, the face veneers have their grain parallel to load and their stiffness is therefore $E_{fL} I_f$, while the core veneer has its grain perpendicular to applied load and its stiffness is $E_{cT} I_c$.

In the tests of ANC-5, Table 2-2, the thickness of one face and of the core veneer was identical and all veneers were made from the same wood species.

The thickness of the three-ply panel is taken as $t = 1$. Then

$$c = .333, f = .667$$

$$I = t^3/12 = {}^1/_{12} \quad (1)$$

$$I_c = .333^3/12 = .003077 \quad (2)$$

$$I_f = I - I_c = {}^1/_{12} - \frac{.333^3}{12} = .080256 \quad (3)$$

$$E_L I = E_{fL} I_f + E_{cT} I_c \quad (4)$$

$$E_T I = E_{fT} I_f + E_{cL} I_c \quad (5)$$

or for the case here under consideration:

$$E_L = E_{fL} (1 - .333^3) + E_{cT} (.333^3) \quad (6)$$

$$E_T = E_{fT} (1 - .333^3) + E_{cL} (.333^3) \quad (7)$$

from these equations the values of the modulus of elasticity of the basic veneers can be calculated now:

$$E_{cL} = E_{fL} = 1.03987\, E_L - .03987\, E_T \quad (8)$$

$$E_{cT} = E_{fT} = 1.03987\, E_T - .03987\, E_L \quad (9)$$

With the above given test values for the three-ply panel, $E_L = 1{,}261{,}000$ lbs. per sq.in., and $E_T = 144{,}000$ lbs. per sq.in., the moduli of elasticity of the basic veneers—African Mahogany—become:

$$E_{cL} = E_{fL} = 1{,}305{,}535 \text{ lbs. per sq.in.} \quad (10)$$

$$E_{cT} = E_{fT} = 99{,}465 \text{ lbs. per sq.in.} \quad (11)$$

For other wood species the moduli of elasticity can be calculated in the same manner from the moduli of elasticity of three-ply panels. Table 2 gives these values of a number of wood species, corrected for moisture content of 12 per cent.

TABLE 2

Moduli of Elasticity of Wood Species. Calculated from Moduli of Elasticity of Three-Ply Panels. Corrected for 12 per cent Moisture Content

Wood Species	Modulus of Elasticity, Lbs. per Sq.In. Parallel to Grain E_L	Perpendicular to Grain E_T	E_L/E_T
Afr. Mahog.	1,320,000	103,800	12.75
Honduras Mahog.	1,276,000	71,750	17.79
Poplar, Yellow	1,508,000	54,000	27.65
Spruce, Sitka	1,360,000	48,000	28.40
Birch, Yellow	2,190,000	97,450	22.50
Basswood	1,181,000	37,300	31.70

Single Veneer under Tension Stress

When a single sheet of wood veneer is stretched by a longitudinal force P, acting parallel to the grain direction of the veneer, it contracts transversely along its width and extends in the direction of the force. The linear strain along the axis of contraction is the decrease of width divided by the original width, and the linear strain along the axis of extension is the increase in length divided by the original length. The ratio of strain along the axis of extension to strain along the axis of contraction is called Poisson's ratio.

Metals have only one value of the modulus of elasticity in tension along all directions of stresses, and they have only one value of Poisson's ratio, since the developed strain at same stress is the same for all directions of stress.

Wood has different moduli of elasticity and therefore different strain values for different directions of tensile stress. Only two of these conditions will be considered: Stress parallel to direction of grain, and stress perpendicular to direction of grain of the wood.

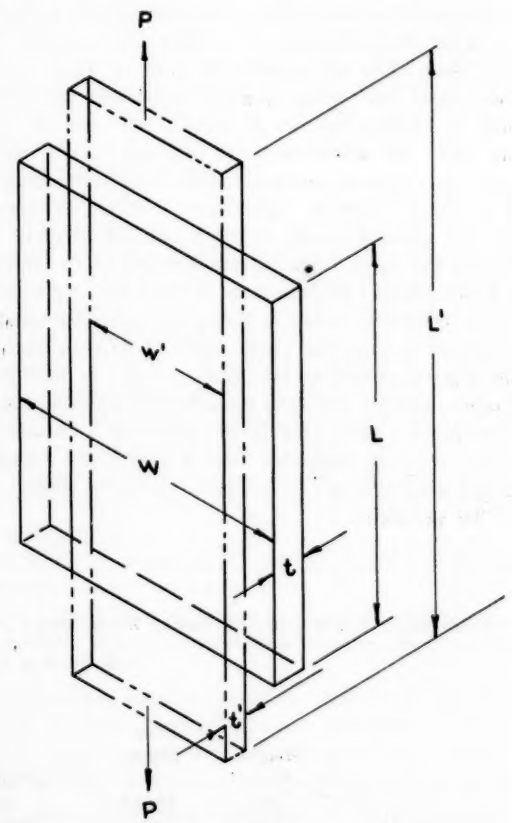

FIG. 1.

A sheet of veneer as shown in Fig. 1, will be assumed to be stressed by a force acting parallel to its grain direction. In the following mathematical procedure, the basic quantities used are defined:

P = Tension force.
p = Tensile stress.
E_L = Modulus of elasticity parallel to the grain of the veneer (longitudinal).
E_T = Modulus of elasticity perpendicular to the grain of the veneer (transverse).
u_L = Poisson's ratio parallel to the grain (longitudinal).
u_T = Poisson's ratio perpendicular to the grain (transverse).
e_L = Strain parallel to grain—that is parallel to applied tensile stress.
e_T = Strain perpendicular to grain—that is perpendicular to applied tensile stress.
L = Length of the veneer parallel to grain before application of stress.
L' = Length of the veneer parallel to grain after application of stress.
W = Width of the veneer perpendicular to grain before application of stress.
W' = Width of the veneer perpendicular to grain after application of stress.
t = Thickness of the veneer before application of stress.
t' = Thickness of the veneer after application of stress.

The elastic constants of the veneer have the following relation, which is required by Maxwell's theorem:

$$\mu_L/E_L = \mu_T/E_T \tag{12}$$

The two axes parallel and perpendicular to the applied stress shall be considered here. There exists a third principal axis perpendicular to the sheet which is not particularly interesting, especially since the thickness of the sheet is assumed to be very small in comparison with its length and width.

With a principal stress applied parallel to the grain the longitudinal extension of the veneer and the longitudinal strain are

$$e_L = (L' - L)/L = P/tE_L = p/E_L \tag{13}$$

The transverse strain or the transverse contraction produced by the longitudinal stress is

$$e_T = (W - W')W = \mu_L p/E_L = \mu_T p/E_T \tag{14}$$

and

$$E_L = p/e_L \tag{15}$$
$$\mu_L = e_T/e_L \tag{16}$$

In wood the principal axes of strain are, in general, not parallel to the principal axes of stress. The relation between axes of strain and axes of stress depends on the angle of grain to axes of stress. In designing aircraft structures made from wood or from wood veneers, the grain direction of the wood must be arranged therefore to take care of this condition, which means that the grain direction must be parallel to applied principal stress.

Three-Ply Panel in Tension

The stresses developed in a three-ply panel in tension shall now be considered. It is assumed that the panel has two face plies of same thickness and of same grain direction, and a core ply whose grain runs at right angle to the face ply grain. The face and core plies are bonded together at their faying surfaces. The tension force acts parallel to the grain of the face plies. Fig. 2 shows such panel.

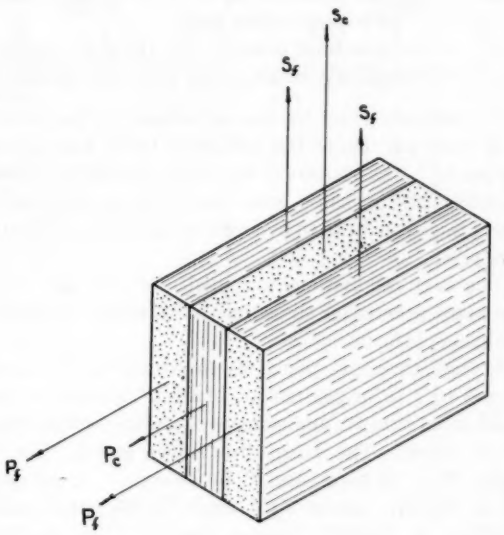

Fig. 2.

In this case the veneers cannot behave as they would if loaded singly. There exists now an interaction between the two face veneers and the core veneer, and all three veneers must extend and contract in unison.

In the mathematical procedure which follows, the constants as defined below are used:

P = External tension stress on three-ply panel.
P_f = Longitudinal stress in face veneers.
P_c = Longitudinal stress in core veneers.
S_f = Transverse stress in face veneer.
S_c = Transverse stress in core veneer.
f = Thickness of face veneers.
c = Thickness of core veneers.
Thickness of panel is unity.
E_{fL} = Modulus of elasticity of face veneers parallel to grain.
E_{fT} = Modulus of elasticity of face veneers perpendicular to grain.
E_{cL} = Modulus of elasticity of core veneer parallel to grain.
E_{cT} = Modulus of elasticity of core veneer perpendicular to grain.
μ_{fL} = Poisson's ratio face veneers parallel to grain.
μ_{fT} = Poisson's ratio face veneers perpendicular to grain.

μ_{cL} = Poisson's ratio of core veneer parallel to grain.
μ_{cT} = Poisson's ratio of core veneer perpendicular to grain.
E_L = Modulus of elasticity of three-ply panel, parallel to face veneer grain.
E_T = Modulus of elasticity of three-ply panel, perpendicular to face veneer grain.
μ_L = Poisson's ratio of three-ply panel parallel to face veneer grain.
μ_T = Poisson's ratio of three-ply panel perpendicular to face veneer grain.
e_L = Longitudinal strain in the three-ply panel.
e_T = Transverse strain in the three-ply panel.

In calculating the stresses developed in the veneers of a three-ply panel the following basic assumptions are made: The veneers of the panel shall all be of same thickness and of same wood species, and the grain of the core veneer is at right angle to the grain of the two face plies.

The first calculations are made for the case where the applied external stress has its direction parallel to the grain of the face plies.

If such three-ply panel, as shown in Fig. 2, is subjected to a principal tension stress P, parallel to face grain, axial strain e_L and transverse strain e_T are produced in the panel. The stress P is shown in Fig. 1 in two parts, P_f in the faces, and P_c in the core. A cut parallel to the axis and at right angle to the panel surface is shown as carrying normal stresses, S_f in the faces, and S_c in the core.

In the three-ply panel in tension, the strain in the panel must equal the strain in each veneer, since the elongation of panel and veneers are identical.

The following relations apply for a general case:

$$fP_f + cP_c = P = 1 \tag{17}$$

$$fS_f + cS_c = 0 \tag{18}$$

$$e_L = (P_f/E_{fL}) - (\mu_{fT}S_f/E_{fT}) = (P_c/E_{cT}) - (\mu_{cL}S_c/E_{cL}) \tag{19}$$

$$e_T = (S_f/E_{fT}) - (\mu_{fL}P_f/E_{fL}) = (S_c/E_{cL}) - (\mu_{cT}P_c/E_{cT}) \tag{20}$$

$$E_L = p/e_L = 1/e_L \tag{21}$$

$$\mu_L = -e_T/e_L \tag{22}$$

The following terms shall now be introduced:

$$K = 1/c;\ \alpha_1 = 1/E_{fL};\ \alpha_2 = 1/E_{fT};$$
$$\beta = \mu_{fL}/E_{fL} = \mu_{fT}/E_{fT};\ \gamma_1 = 1/E_{cL};$$
$$\gamma_2 = 1/E_{cT};\ \delta = \mu_{cL}/E_{cL} = \mu_{cT}/E_{cT}.$$

The relations become then:

for Eq. (17): $P_c = K - KfP_f$ (23)

for Eq. (18): $S_c = -KfS_f$ (24)

$$e_L = \alpha_1 P_f - \beta S_f = \gamma_2 P_c - \delta S_c \tag{25}$$

$$e_T = \alpha_2 S_f - \beta P_f = \gamma_1 S_c - \delta P_c \tag{26}$$

$$e_L = K\gamma_2 - Kf\gamma_2 P_f + Kf\delta S_f = \alpha_1 P_f - \beta_2 S_f \tag{27}$$

$$S_f = [P_f(\alpha_1 + Kf\gamma_2)/(\beta_2 + K_f\delta)] - [K\gamma_2/(\beta_2 + Kf\delta)] \tag{28}$$

$$e_T = \alpha_2 S_f - \beta_1 P_f = -Kf\gamma_1 S_f - K\delta + Kf\delta P_f \tag{29}$$

$$S_f = [(\beta_1 + Kf\delta)P_f/(\alpha_2 + Kf\gamma_1)] - K\delta/(\alpha_2 + Kf\gamma_1) \tag{30}$$

Eqs. (28) and (30) can now be used to evaluate P_f.

$$P_f = \frac{\dfrac{K\gamma_2}{\beta_1 + Kf\delta_1} - \dfrac{K\delta}{\alpha_2 + Kf\gamma_1}}{\dfrac{\alpha_1 + Kf\gamma_2}{\beta_1 + Kf\delta} - \dfrac{\beta_1 + Kf\delta}{\alpha_2 + Kf\gamma_1}} \tag{31}$$

This makes it possible to find S_f, e_L and e_T. Then:

$$E_L = 1/e_L \text{ and } \mu_L = -e_T/e_A.$$

If the face and core materials are identical, the following relations apply:

$$\alpha_1 = 1/E_{fL} = \gamma_1 = 1/E_{cL} = a$$
$$\alpha_2 = 1/E_{fT} = \gamma_2 = 1/E_{cT} = b$$
$$\beta = \delta = d \quad (\mu_{fL}/E_{fL} = \mu_{fT}/E_{fT} = \mu_{cL}/E_{cL} = \mu_{cT}/E_{cT})$$

Eq. (31) becomes for this panel:

$$P_f = \frac{\dfrac{Kb}{d(1 + Kf)} - \dfrac{Kd}{b + Kfa}}{\dfrac{a + Kfb}{d\ (1 + Kf)} - \dfrac{d(1 + Kf)}{b + Kfa}} \tag{32}$$

For a panel made of African Mahogany veneers, the values of Poisson's ratio for the basic wood specie are given by Jenkins,[4] page 105. These values are: For quarter-sliced veneers

at stress parallel to grain $\mu_L = .312$
at stress perpendicular to grain $\mu_T = .0241$

For the three-ply panel of African Mahogany, the constants used in Eq. (32) are:

$K = 1/c = 1/.333 = 3.00$
$a = 1/E_L = 1/1{,}304{,}240 = .0000007667$
$b = 1/E_T = 1/100{,}760 = .000009925$
$d = \mu_L/E_L = .312/1{,}304{,}240 = .000000239$
$f = .667$

With these constants the stresses in the face plies can now be calculated

$$P_f = 1.446$$

From Eq. (23) the stress in the core ply is evaluated as

$$P_c = K - KfP_f = .1109$$

Therefore:

$$P_f/P_c = 1.446/.1109 = 13.03$$

ANC-5, Table 2-2,[3] give results of tests on such three-ply panels of African Mahogany veneers. For loads applied parallel to face grain, the average value of tensile strength is given at 5370 lbs. per sq. in.

$2F_{fT} + (1/13.03)F_{fT} = 3 \times 5370$ lbs. per sq.in.

The stress in the face plies is

$$F_{fT} = 7770 \text{ lbs. per sq.in.}$$

and the stress in the core ply is

$$F_{cT} = 7770/13.03 = 596 \text{ lbs. per sq.in.}$$

If the stress on the panel is applied parallel to the grain of the core veneer, the values for P_f and P_c are reversed, $P_f = .1109$ and $P_c = 1.446$. $P_c/P_f = 13.03$, and the stresses in the veneers are, for a total tensile strength of the three-ply panel of 3770 lbs. per sq.in.:

$$F_{cT} + (2/13.03)F_{cT} = 3770 \times 3$$

The stress in the core ply is then

$$F_{cT} = 9820 \text{ lbs. per sq.in.}$$

and the stress in the face plies is

$$F_{fT} = 753 \text{ lbs. per sq.in.}$$

This shows that the stresses for all plies depend on the location of the ply in the three-ply panel and on the interaction between plies that have their grain parallel or perpendicular to the applied panel stress.

This may be checked by a short-cut method for various panels and appears to hold true for the data on three-ply panels given in ANC-5, Table 2-2.[3]

The ratio between stresses in face and core plies is for the Mahogany panel 13.03, which is also the ratio between the longitudinal and transverse moduli of elasticity.

Considering the same three-ply African Mahogany panel, the values of EA are for tension loading parallel to face grain:

for the faces EA	$= (^2/_3) \times 1{,}304{,}240 =$	870,000
for the core EA	$= (^1/_3) \times 100{,}760 =$	33,600
for the panel EA	$=$	903,600

This value of EA is also the value of the apparent modulus of elasticity in tension, since the cross-section area of the panel is taken as unity.

Under the maximum tensile stress of 5370 lbs. per sq.in. for the panel, the strain becomes 5370/903,600 = .00595, and the stresses in the plies are

for the faces $1{,}304{,}240 \times .00595 = 7770$ lbs. per sq.in.
for the core $100{,}760 \times .00595 = 596$ lbs. per sq.in.

These values check with those previously obtained.

For loading perpendicular to face grain the values of EA are

for the faces EA	$= (^2/_3) \times 100{,}760 =$	67,100
for the core EA	$= (^1/_3) \times 1{,}304{,}240 =$	434,750
for the panel EA	$=$	501,850

Under the maximum stress for the panel of 3770 lbs. per sq.in., the strain for the panel is 3770/501,850 = .00752, and the stress in the plies are:

for the faces $100{,}760 \times .00752 = 753$ lbs. per sq.in.
for the core $1{,}304{,}240 \times .00752 = 9820$ lbs. per sq.in.

These values of stresses in the veneers appear to be of a rather interesting nature and they shall be illustrated in Fig. 3, where the three-ply panel is shown in cross-section, with stresses given for each of the plies for the two conditions of loading.

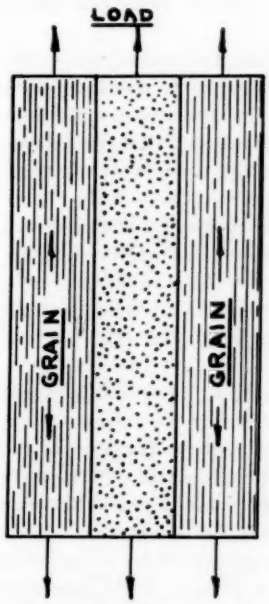

FIG. 3a. Stresses in plies of three-ply panel under tension load, load parallel to face grain. Stresses in lbs. per sq.in.: faces, 7700 each; core, 596; entire panel, 5370.

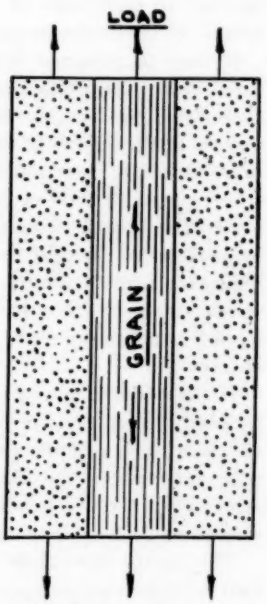

FIG. 3b. Stresses in plies of three-ply panel under tension load, load parallel to core grain. Stresses in lbs. per sq.in.: faces, 753 each; core, 9820; entire panel, 3770.

An inspection of Fig. 3 shows that the longitudinal stress for the veneer increases from 7770 lbs. per sq.in. when the veneer is located at the outside of the panel to 9820 lbs. per sq.in., when the veneer is at the center of the three-ply panel, an increase of 26.4 per cent. Such increase cannot be explained by variations in the thickness of plies of the test panels, and furthermore, the data given in Table 2-2 of ANC-5,[3] are the average of 20 tests on African Mahogany panels as carried out by the U.S. Department of Agriculture, Forest Products Laboratory, at Madison, Wisconsin. The higher one of these stresses, 9820 lbs. per sq.in., approaches the modulus of rupture value of African Mahogany, which is 10,800 lbs. per sq.in., while the lower value of longitudinal tensile stress for these veneers, 7770 lbs. per sq.in., is 28 per cent below the value of modulus of rupture.

The reason for these large variations of stresses in the veneers might be the fact that any chain is only as strong as its weakest link. Although the transverse

veneers carry only small percentages of the total panel load, any failure in those transverse veneers would throw the total load suddenly into the longitudinal veneers, which would make them fail suddenly. It can be noted from static tests of three-ply panels that they fail by splitting at right angles to the face grain, that is parallel to core grain, if the faces are at the outer side of the panel. If single veneers are tested in tension, the failure has a much more ragged appearance, with many long slivers extending finger-like from the breakage line to both ends of the veneer along the grain, with short transverse breaks.

It may be assumed that the transverse veneer located at the centerline of the three-ply panel is pulled at both of its face surfaces by the two longitudinal veneers at the outside of the panel, and that the elongation induced in these longitudinal veneers creates peak stresses at both ends of the cross-section of the transverse core veneer. These two peak stresses may well have the effect to split the transverse veneer along its grain, whereby the entire tension load would be transferred suddenly into the longitudinal veneers, which causes panel failure at comparatively low average stresses.

If the transverse veneers are at the outside of the three-ply panel, these peak stresses would occur only at one face surface of the veneer and the ductility of the material enables the veneer to distribute this peak stress over the cross-section, whereby the transverse veneer would be able to carry higher stresses.

This entire case might be simulated by considering two splitting operations on a piece of wood, one with two knives acting from both ends toward the middle, the other with one knife acting at one end only. The two-knife action would split this piece more easily.

Tests carried out on multi-ply panels appear to strengthen this theory. Nine-ply panels made of African Mahogany gave an average tensile strength of 5320 lbs. per sq.in., corrected for 12 per cent moisture content. Five laminations had longitudinal grain, that is parallel to direction of load, the other four laminations had transverse grain. According to the test results as shown in Fig. 3, the transverse grain veneers carry a stress of 600 lbs. per sq.in., since all are located between two longitudinal veneers.

The stresses for the two longitudinal veneers at face and back of the panel carry 7770 lbs. per sq.in., and the three other longitudinal veneers, located inside the panel, carry a tensile stress of 9820 lbs. per sq.in.

For the total panel, the tensile stress is then $[(4 \times 600) + (2 \times 7770) + (3 \times 9820)]/9 = 5267$ lbs. per sq.in., which is surprisingly close to the test results.

By the method given here, tensile strength values have been calculated for several wood species on the basis of data for three-ply panels. These tensile strength values do not agree entirely with the modulus of rupture values of Table 1, even when those values are adjusted to 12 per cent moisture content. It appears, however, that these values, which are given in Table 3, can be used for strength determination of multi-ply panels of wood veneers, since these values are giving somewhat conservative results. Care must be taken to use the proper values for veneers that are at the faces or at the inside of these panels.

The dimensions of the skin material of stressed-skin wings, fuselages, tail surfaces, and the like are usually determined from compression stresses occurring for the various conditions of flight, and the skin panels designed to be stiff enough in compression will usually have a high margin of safety for tension loads.

Compression Stresses

Wood-veneer base materials are very well suited for construction of shells for fuselages, wing and other parts of aircraft, and they appear to be up to now, the only type of material that can be used in molded panel form without any or with only a very small number of longitudinal stiffeners.

In all cases of designing for compression loads, the stiffness of the stressed skin is based on the product of moment of inertia, times the modulus of elasticity of the material. A material of low density can be used to make up thicker panels than possible for a material of high density, if the weight of both panels is to be the same. The lower modulus of elasticity of the material

Table 3

Tensile Strength of Laminations in Multi-Ply Constructions. Calculated from Tensile Strength Data of Three-Ply Panels of Table 2-2 of ANC-5.[3]
Corrected for 12 Per Cent Moisture Content

	Tensile Strength, Lbs. per Sq.In.			
	Veneers at Face of Panel		Veneers Inside of Panel	
Wood Species	Parallel to Grain	Perpendicular to Grain	Parallel to Grain	Perpendicular to Grain
Afr. Mahog.	7,950	787	10,000	625
Honduras Mahog.	9,100	560	9,950	513
Poplar, Yellow	9,950	432	12,050	356
Spruce, Sitka	7,200	280	7,950	254
Birch, Yellow	16,400	802	18,000	730

TABLE 4

Calculation of Apparent Modulus of Elasticity for a Nine-Ply Panel of African Mahogany

Grain	t	y	y^2	ty^2	E	$ty^2 \times E$
L	.0311	.1244	.01545	.00482	1,300,000	626.0
T	.0311	.0933	.00870	.000272	100,000	27.2
L	.0311	.0622	.00386	.000120	1,300,000	156.0
T	.0311	.0311	.00097	.000030	.....	3.0
Outer Plies	.1244	...	.....	.000904	.....	812.2
L (Core)	.0311	...	.....	....	.....	
Outer Plies	.1244	...	.....	.000904	.....	812.2
	.2799	...	.....	.001808	.....	1624.4
L 5 ×	...	...	$.0311^3/12$	.000013	1,300,000	16.9
T 4 ×	...	...	$.0311^3/12$	.000010	100,000	1.0
				I = .0001831		EI = 1642.3

of low density is thereby more than compensated in most cases.

A wing shall have, for example, a skin of aluminum alloy of .040 inch thickness without any longitudinal stringers. The stiffness of the skin is then

$$EI = 10{,}000{,}000 \times .040^3/12 = 53.3 \text{ in. lbs. in.}$$

A wing skin made of Mahogany base Duramold having a specific gravity of .54, can have, for same weight as the metal skin, a thickness of $.040 \times 2.8/.54 = .2075$ inch. The effective longitudinal modulus of elasticity of such Duramold skin, having 70 per cent of the veneers with grain in direction of the load, is approximately $E_L = 1{,}000{,}000$. The value of this effective modulus of elasticity varies with varying percentages of longitudinal and transverse grain of the veneers of the panel, as will be outlined later on.

The stiffness of such Duramold panel is then

$$EI = 1{,}000{,}000 \times .2075^3/12 = 744 \text{ in. lbs. in.}$$

The stiffness of this Duramold skin is therefore 13.9 times that of the aluminum alloy skin of same weight. This explains partially why it is possible to build shells of wood-veneer base laminations without reinforcing them by a multitude of stringers. If this wing skin is assumed to be made of all-birch laminations, having a specific gravity of about .76, it could have a thickness of $.040 \times 2.8/.76 = .147$ inch to be of same weight as the previously considered aluminum alloy and Mahogany base skin. The apparent modulus of elasticity of the panel is $E_L = 1{,}350{,}000$ lbs. per sq.in., based on same number and distribution of laminations as used for the Mahogany base panel and on a basic modulus of elasticity of $E_L = 1{,}960{,}000$ lbs. per sq.in., for the longitudinal veneers and of $E_T = 130{,}000$ lbs. per sq.in., for the transverse veneers.

The stiffness of this birch-base skin is then $EI = 1{,}350{,}000 \times .147^3/12 = 310$ in. lbs. in., which is only 5.8 times that of the aluminum alloy skin.

For same weight the Mahogany base shell is therefore far superior to the birch-base shell in compressive strength and in local stiffness. The higher value of the moduli of elasticity of the basic veneers of birch is more than offset by the lesser thickness of the birch skin, required for same weight.

The calculation of apparent modulus of elasticity in compression is carried out in Table 4 for a panel constructed of nine laminations for $^1/_{32}$ inch African Mahogany veneer. Five of these laminations have the grain in direction of the compression load, the other four laminations have the grain perpendicular to the load.

The basic moduli of elasticity of the veneers are assumed to be

E_L (longitudinal) = 1,300,000 lbs. per sq.in.
E_T (transverse) = 100,000 lbs. per sq.in.

The moment of inertia of each ply is:

$$I_{\text{ply}} = ty^2 + t^3/12$$

where y is the distance of the ply centerline from the panel centerline and t is the thickness of the ply.

I = .0001831 in.^{4} (per inch)
EI = 1642.3 in.^{2} lbs.
apparent E_L = 1642.3/.0001831 = 897,000 lbs. per sq.in.

This value of apparent E_L checks very well with the measured longitudinal modulus of elasticity of such panels from compression tests.

The apparent modulus of elasticity can be used to calculate the compression strength of flat panels, whereby the conditions of end- and of side-restraint must of course be taken into consideration. Panels used in aircraft construction should usually be considered to be simply supported at the edges.

The calculations become somewhat more complex when curved laminated panels under compression loads are considered. Such panels can be considered as parts of a cylinder. Ballerstedt and Wagner,[5] page 309, give an equation for allowable compression stresses for thin-walled metal cylinders,

$$F_c = (.2Et/R) + (KE(t/L)^2) \quad (33)$$

where E = Modulus of elasticity.
t = Wall thickness of the cylinder.
R = Radius of curvature.
L = Length of cylinder.

This equation has been proved by Ballerstedt and Wagner,[5] by tests on metal cylinders of $L/R = .25$ to 2.0 and $t/R = 1/250$ to $1/4000$. The coefficient K is 3.3 for cylinders with built-in end frames. If the ends of the cylinder shell are only resting on a plate, this coefficient is $K = .83$.

Introducing the term $t^3/12$ in this equation, that is the moment of inertia for a strip of the cylinder wall of one inch width, Eq. (33) becomes

$$F_c = (2.4EI/Rt^2) + (4\pi^2 EI/L^2t) \quad (34)$$

The second term of this equation evidently represents Euler's formula for the strength of a long column with fixed ends. The first term represents an effect that is due to the lateral support which is provided by the connection of all the longitudinal strips of the cylinder wall together at their edges, that is therefore the hoop strength of the cylinder.

For an isotropic material only one value of the modulus of elasticity is usually considered for different directions of loadings and of reactions. For laminated materials, as for instance the wood-base laminations here considered, two distinctly different moduli of elasticity must be used: the modulus of elasticity in tension, which is a function of the cross-section area of each lamination times the pertaining modulus of elasticity of this lamination, E_A, and the modulus of elasticity in compression, which is a function of the moment of inertia of each lamination about the neutral axis of the panel times the pertaining modulus of elasticity of the lamination, E_I.

It is obvious that E_A should apply for the first term, since the strength derived from lateral support is a function of tension, and that E_I applies to the Euler term of the equation.

Tests made by Duramold Aircraft Corporation indicate that Eq. (34) reads for cylinders of cross-laminated material under straight compression loads

$$F_c = (2.2\,E_AI/Rt^2) + (3.3\pi^2E_II/L^2t) \quad (35)$$

Lundquist,[6] gives for thin-walled duralumin cylinders, the buckling stress at failure as

$$F_c = K_cE \quad (36)$$

Values of the factor K_c for Duramold cylinders in compression have been calculated from test data and are given in Table 3. The test cylinders were all made of three-ply construction with African Mahogany longitudinal face and back veneers and with Yellow Poplar transverse core veneers. The value of E_L is used in Eq. (4) for these cylinders.

Values of K_c for Duramold cylinders can be plotted in the same manner as given by Lundquist,[6] Fig. 9. The values appear to follow similar lines to those given in that figure and lie to the left and above the values for the duralumin cylinders, that is K_c is higher for the Duramold cylinders of smaller radius-over-thickness ratio than that of the duralumin cylinders.

The larger influence of length-over-radius ratio for the Duramold cylinders seems to indicate that the use of Eq. (35) given in this paper is preferable to the use of the factor K_c and of equation $F_c = K_cE_I$, when compression strength cylinders is to be determined.

TABLE 5

Duramold Cylinders in Compression

$F_c = K_cE$ (Eq. of ref.[6])

Cylinders Group A

$R = 10$ inches, $t = .10$ inch, $R/t = 100$

Face veneer thickness 60 per cent, $E_I = 1{,}250{,}000$ lbs. per sq.in.

L inches	40	20	10	5
L/R	4	2	1	.5
K_c	.00098	.00108	.00133	.00202

Cylinders Group B

$R = 10$ inches, $t = .075$ inch, $R/t = 133.3$

Face veneer thickness 50 per cent, $E_I = 1{,}160{,}000$ lbs. per sq.in.

L inches	40	20	10	5
L/R	4	2	1	.5
K_c	.00102	.00110	.00123	.00185

Cylinders Group C

$R = 10$ inches, $t = .141$ inch, $R/t = 71.0$

Face veneer thickness 66 per cent, $E_I = 1{,}270{,}000$ lbs. per sq.in.

L inches	40	20	10	5
L/R	4	2	1	.5
K_c	.001275	.00141	.00174	.00326

Application of Stress Data and Methods to Design Stabilizer for Fairchild Low-Wing Trainer

By use of the stress analysis methods described here and based on a long series of tests and investigations, a number of aircraft structures have been designed, constructed and tested by Duramold Aircraft Corporation.

One of these designs is the stabilizer for the Fairchild M-62 low-wing training plane. This stabilizer is a stressed-skin type without longitudinal stringers and without a front spar. It consists merely of molded top and bottom shells, whose thickness tapers from approximately $^1/_4$ inch at the centerline of the airplane to $^3/_{32}$ inch at the stabilizer tip, of a light rear spar that takes vertical shear and is used for the attachment of elevator and fuselage fittings, of a leading-edge-former that curves in one part into the tip bows, and of a few chordwise ribs. The shell is, on account of its

thickness, a very stiff one and assures the maintenance of the proper airfoil section under all conditions of flight loads. In combination with the remainder of the structure it assures very high torsional stiffness, and load tests have shown that the torsional twist of this stabilizer was only .50 degree under full design load, consisting of the pertaining stabilizer-down and elevator-up loads. The complete weight of this Duramold stabilizer is the same as of the plywood-plus-spars type of the original design.

The stress analysis of this stabilizer was made by calculating for several chordwise sections the moments of inertia of the shell section and by determining from the loading curves the bending, shear and torsion stresses for these sections. The allowable stresses for the shell sections were calculated by the methods given previously in this paper. For compression stresses the allowable stresses were calculated by taking the curvature of the shell into consideration, as well as the shell thickness, the method of shell veneer lay-up and the rib spacing. For each section the mean radius of curvature was determined and this radius was used in Eq. (35) of this paper for determination of the allowable stresses. The values of E_A and E_I of Eq. (35), were, of course, evaluated as given previously in this paper. The term L in the second part of Eq. (35) is the rib spacing, since tests on short cylinders with total length L between end rings and tests on long cylinders with spacing L between intermediate stiffener rings gave same compression strength. Tension stress allowables were calculated also by the method as given here on preceding pages. Shear center for several stations of this stabilizer was calculated by the method given by Newell.[7]

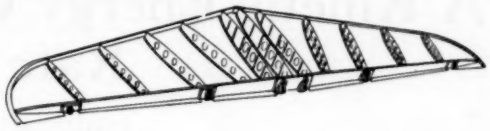

FIG. 4.

Fig. 4 shows the lower shell of this stabilizer with bonded-in rear spar, leading-edge-tip-bow, and ribs. A molded top shell is bonded to this assembly.

Rib capstrips are made of laminated construction and they are bonded to the shells. Rib webs of flat plywood type with occasional vertical stiffeners are bonded into grooves of these rib capstrips.

REFERENCES

[1] Markwardt, L. J., *Aircraft Woods: Their Properties, Selection and Characteristics*, N.A.C.A. Report No. 354, Reprint U.S. Department of Agriculture, Forest Products Laboratory, Report No. 1079, October, 1941.

[2] Trayer, G. W., *Wood in Aircraft Construction*, published by the National Lumber Association, Washington, D. C., 1930.

[3] *Strength of Aircraft Elements*, Report ANC-5, issued by the Army-Navy-Commerce Committee on Aircraft Requirements, Washington, D. C., January, 1938.

[4] Jenkins, C. F., *Materials of Construction Used in Aircraft*, Aeronautical Research Committee (British) Report, 1920.

[5] Ballerstedt, W., and Wagner, H., *Tests on the Strength of Thin-Walled, Non-Reinforced Cylinders in Shear and in Compression*, Luftfahrtforschung, Volume 13, No. 9, Berlin, Sept. 20, 1936.

[6] Lundquist, Eugene E., *Strength Tests of Thin-Walled Duralumin Cylinders in Compression*, N.A.C.A. Report No. 473, Washington, D. C., 1933.

[7] Newell, Joseph S., *The Analysis of Leading-Edge Wing Beams*, S.A.E. Journal, September, 1939.

A Kinetic Energy Correction to Predicted Rate of Climb

FREDERICK C. PHILLIPS

Glenn L. Martin Company

SUMMARY

The assumption of zero acceleration along flight path, generally made in the interest of simplification in climb performance calculations, is pointed out, and the general performance equation re-stated for the case of finite acceleration. This assumption is shown to result in optimistic predicted rates of climb. The percentage error involved is analyzed and shown to increase rapidly with airplane loading and with altitude, particularly in the stratosphere.

The war emergency is accelerating tremendously the trend toward higher operating altitudes and higher loadings for military aircraft. Increasing climb errors involved by these trends will shortly be of appreciable magnitude. The case of a high altitude bomber is given to illustrate quantitatively. It is recommended that allowance be made, in establishing climb performance guarantees and in correlating computed and flight rates of climb, for the error incurred by assumption of zero acceleration along the flight path.

INTRODUCTION

THE PRESENT EMERGENCY, by particularly emphasizing military airplane performance, is a stimulus toward development of more precise performance methods. Decreasing tolerances of error have pointed out weaknesses in methods that previously were considered to give satisfactory correlation between computed and flight performance data. Further weaknesses are becoming noticeable because a number of variables are rapidly tending to be critical—wing and propeller loadings, engine installation, Mach numbers of component parts. For airplanes of even the near future the present methods cannot be expected to achieve correlation as satisfactory as in the past. The fundamentals of performance methods must be reviewed in the light of future design conditions and strengthened where needed, lest future flight data fall short of expectation.

This paper reviews the fundamental performance equation with the purpose of pointing out a correction to computed rate of climb that may be expected to become appreciable shortly.

SYMBOLS

The following symbols will be used:

F	= force in general
W	= gross weight (lb.)
T	= thrust (lb.)
D	= drag (lb.)
a	= acceleration (ft. per sec.^{2})
g	= acceleration of gravity
θ	= inclination of flight path to horizontal (radians)
C	= flight rate of climb (ft. per sec.)
C'	= computed rate of climb without kinetic error correction
V_c	= airspeed along flight path in climb
V	= airspeed along flight path
V_{ci}	= indicated airspeed along flight path in climb
t	= time (sec.)
t_c	= time to climb (min.)
E	= kinetic energy (ft.lbs.)
A	= horsepower equivalent (550 ft.lbs. per sec.)
P_a	= thrust horsepower available
P_r	= thrust horsepower required
η	= propulsive efficiency
b.hp.	= total airplane brake horsepower
ρ	= air mass density (slugs per cu.ft.)
f	= airplane drag area (sq.ft.)
R	= geometric aspect ratio
e	= Oswald airplane efficiency factor
b	= wing span (ft.)
h	= altitude (ft.)
C_L	= airplane lift coefficient
C_D	= airplane drag coefficient
C_{D_p}	= $C_D - (C_L^2/\pi eR)$

DEVELOPMENT

Consider the summation of forces ΣF_D acting on the airplane along the flight path, as shown in Fig. 1. The forces are shown as concurrent and the thrust force, T, is assumed parallel to the flight path—both valid assumptions for the purpose of the summation in question.

$$\Sigma F_D = (W/g)a = T - D - W \sin\theta \qquad (1)$$

$$W[\sin\theta + (a/g)] = T - D \qquad (1a)$$

In terms of work, and since $\sin\theta = C/V$,

$$WV[(C/V) + (1/g)(dV/dt)] = (T - D)V \qquad (1b)$$

$$WC + (W/g)[d(V^2/_2)/dt] = WC + (dE/dt) = A(P_a - P_r) \qquad (2)$$

Presented at the Aerodynamics session, Tenth Annual Meeting, I.Ae. S., New York, January 30, 1942.

In general terms, then, the familiar performance equation can be written from the above, assuming $L = W$, and Munk's span factor unity (for monoplanes):

$$WC + (dE/dt) = A\eta(\text{b.hp.}) - (\rho/2)fV^3 - [W^2/\pi(\rho/2)eb^2V] \quad (3)$$

This equation is usually shown without the term dE/dt, and climb calculations are usually made neglecting this dynamic effect. The error involved in climb calculations by this procedure can become appreciable, as investigation will point out.

Eq. (2) can be rewritten as:

$$C + (V_c/g)(dV_c/dt) = (A/W)(P_a - P_r) \quad (2a)$$

Ordinarily the kinetic term is neglected and climb calculations are made using:

$$C' = (A/W)(P_a - P_r) \quad (2b)$$

Hence $(V_c/g)(dV_c/dt) = (1/W)(dE/dt) = C' - C = \Delta C$, the error in computed rate of climb. The decimal error $\Delta C/C = (V_c/gC)(dV_c/dt)$, but since $C = dh/dt$, then

$$\Delta C/C = (V_c/g)(dV_c/dh) \quad (4)$$

With V_c in m.p.h., and $g = 32.2$, Eq. (4) becomes

$$\Delta C/C = .0667\ V_c(dV_c/dh) \quad (4a)$$

Rate of climb calculations made using Eq. (2b) should be corrected for the error of Eq. (4a): $C = [C'/1 + (\Delta C/C)]$.

Discussion

Best rate of climb tends to occur at a constant indicated airspeed (constant C_L operation) regardless of altitude, this speed being slightly above the speed for minimum power required ($C_D = 4C_{D_p}$ and $C_L = \sqrt{3\pi C_{D_p} eR}$). Because of this tendency, which necessitates increase in true airspeed with altitude and loading, the error as given by Eq. (4) would appear to increase likewise, although the altitude variation of dV_c/dh is not obvious.

Eq. (4) has greater significance when expanded in terms of indicated airspeed. Substitution of $V_c = V_{ci}/\sqrt{\sigma}$ gives upon expansion:

$$\Delta C/C = 1/2g[V_{ci}^2 d(1/\sigma)/dh + 1/\sigma d(V_{ci}^2)/dh] \quad (5)$$

$$\Delta C/C = V_{ci}^2/2g[d(1/\sigma)/dh] + V_{ci}/g\sigma[dV_{ci}/dh] \quad (5a)$$

Again, with V_c in m.p.h. and $g = 32.2$:

$$\Delta C/C = V_{ci}^2\gamma + (.0667/\sigma)V_{ci}(dV_{ci}/dh) \quad (5b)$$

where $\gamma = .0333\ d(1/\sigma)/dh$ (Fig. 2). The first term of Eq. (5b), fixed by indicated speed and altitude, constitutes the entire error when indicated climb speed is constant. The gradient of V_{ci} against h, required in the second term of the equation, is a function of combined engine power and propeller characteristics.

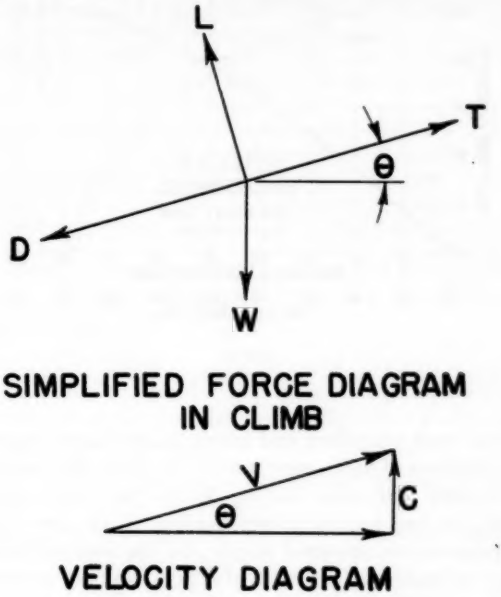

Fig. 1.

Although it is often difficult to generalize, constant power engine operation, by serving to load the propeller more heavily with increasing altitude, acts to maintain a constant indicated speed; under full throttle operation V_{ci} will ordinarily decrease, making dV_{ci}/dh negative. High propeller loadings realized in small propellers favor higher climbing speeds and maintenance of constant V_{ci}.

The desire to obtain good climb performance at high altitudes has brought about the combination of rela-

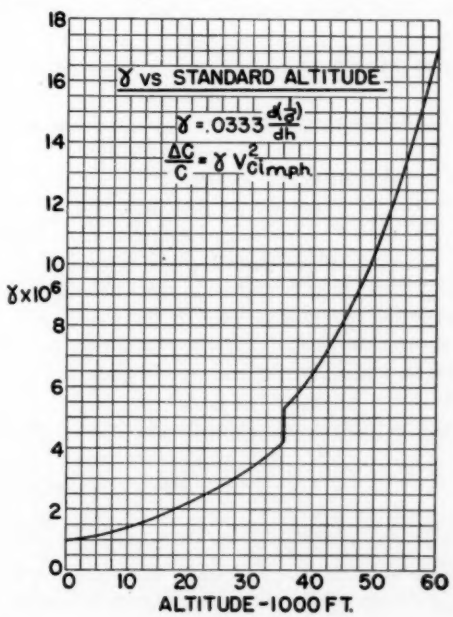

Fig. 2.

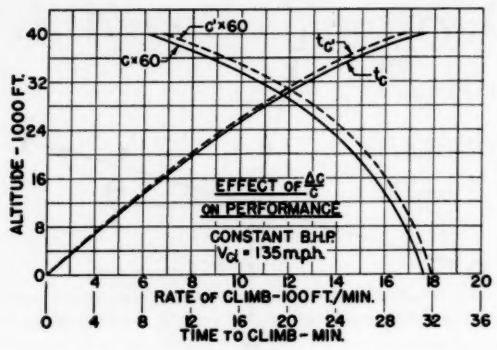

FIG. 3.

tively large propellers and highly supercharged engines in airplanes of high aspect ratio. A study was made of a bomber with wing loading 50 lbs. per sq.ft., aspect ratio 10, and normal power loading 10 lbs. per b.hp. A propeller was selected to give, for the constant power high altitude engines used, the best climbing performance possible without unduly penalizing other performance items, for example, high speed. Calculations showed that for this airplane, the indicated climbing speed remained constant at 135 m.p.h. from sea level to 40,000 feet. Rates of climb were computed by the usual method, Eq. (2b); time to climb was calculated from these rates of climb. These data are the dashed lines of Fig. 3. The dynamic climb error of Eq. (5b), without the second term, was computed at several altitudes and the previous rates of climb corrected. The revised data are shown in solid lines as is the new time to climb curve. The discrepancies in rates of climb due to the correction for dynamic error are only 2 per cent at sea level, but 11 per cent at 40,000 feet. These errors in rates of climb cause an error of 6 per cent in time to climb to 40,000 feet. It is to be noted that these errors make computed figures optimistic.

In the case of a high altitude fighter of wing loading 40 and aspect ratio 8, with constant-power engine, the dynamic errors in climb are approximately those given above for the bomber.

CONCLUSIONS

Present tendencies in airplane development are toward extremely high altitude operation as fast as supercharging techniques will allow. Climbing performance at these altitudes is of critical importance; rate of climb at critical altitude and time to climb to high altitude are becoming guarantee items of importance along with the customary service ceiling. Because of the appreciable error of optimism introduced in predicted climb data by neglecting the kinetic term, the correction developed here should be made to computed data, particularly when establishing guarantees.

Further, when investigating correlation between computed and flight test climb data, the kinetic error as fixed by the flight climb speed schedule should be subtracted from computed rates of climb otherwise comparable to corrected flight data.

The Lateral Instability of Unsymmetrical I Beams

H. N. HILL*

Aluminum Company of America

SUMMARY

An expression is derived for calculating the critical bending moment at which lateral buckling will occur in an I beam which is unsymmetrical about the principal axis normal to the web. The expression is derived for the case in which the beam is subjected to pure bending. This problem differs from the similar problem involving the buckling of beams of symmetrical I cross-section in that the shear center of the section does not coincide with the center of gravity.

Experimental verification of the expression is obtained from the results of tests made to study the lateral buckling of unsymmetrical aluminum alloy I beams under pure bending.

INTRODUCTION

UNDER CERTAIN conditions of loading and restraint, beams may fail by the compression flange buckling sidewise in much the same manner as columns buckle under axial compressive loads. Despite the similarity of the nature of the failure in the beam and the column, the problem of the lateral instability of flanged beams cannot be solved simply by considering the column strength of the compression flange. This approach to the problem neglects one very important element—the torsional stiffness of the beam.

The problem of the lateral instability of symmetrical I beams under various conditions of loading and restraint has been dealt with at considerable length.[1, 2, 3] Design formulas[4, 5] for determining allowable compressive bending stresses for flanged beams have been derived on the basis of theoretical solutions of this problem.

Beams are sometimes encountered which have an I cross-section symmetrical about an axis in the web, but have no axis of symmetry normal to the web; such, for instance, as an I beam having flanges of unequal widths. The resistance of such a beam to lateral buckling will depend on whether the wide or the narrow flange is in compression. A consideration of the lateral stability of such beams under pure bending provides the subject for this paper.

Presented at the Structures (Part 1) session, Tenth Annual Meeting, I.Ae.S., New York, January 28, 1942.

* The material presented in this paper was accepted as a thesis by the University of Pittsburgh as partial fulfillment of the requirements for a technical degree. The author wishes to acknowledge his indebtedness to Mr. R. L. Templin of the Aluminum Research Laboratories, under whose supervision the work was done, and to Mr. C. Dumont of the same organization, who conducted the tests.

SYMBOLS

The following symbols are used in the analytical treatment of this problem:

M = bending moment applied in the plane of the web of an I beam

M_{cr} = critical bending moment (at which lateral buckling occurs)

N = lateral restraining moment at ends of unsupported length (see Fig. 1)

E = modulus of elasticity

G = modulus of rigidity

$$G = E/2(1 + \mu)$$

μ = Poisson's ratio

h = height of beam (distance between centers of flanges) (see Fig. 2)

a = distance between shear center and center of flange A (see Fig. 2)

b = distance between shear center and center of flange B (see Fig. 2)

e = distance between shear center and centroid of the section (see Fig. 2)

I_A = moment of inertia of flange A about principal axis in the web

I_B = moment of inertia of flange B about principal axis in the web

I_Z = moment of inertia of cross-section about principal axis in the web

J = section factor for torsion

L = laterally unsupported length

n = a coefficient denoting the degree of lateral restraint at the ends of the laterally unsupported length. If the ends are free to rotate about an axis in the plane of the web and normal to the flange, $n = 1$. If the ends are completely restrained against such rotation, $n = 2$

θ = angle of twist

ANALYTICAL TREATMENT

As was previously stated, the resistance of an I beam to lateral buckling depends on the torsional stiffness of the beam as well as on its flexural stiffness in the

lateral direction. If an I beam is restrained at both ends and subjected to a torque at the middle, twisting of the beam about its longitudinal axis is accompanied by bending of the flanges. It is therefore necessary to consider the bending resistance of the flanges in determining the torsional resistance of the beam.[2]

The critical bending moment for a symmetrical I beam loaded in the plane of the web and subjected to pure bending can be expressed[2]

$$M_{cr} = \frac{n^2\pi^2 EI_Z}{L^2}\sqrt{\frac{L^2GJ}{n^2\pi^2 EI_Z} + \frac{h^2}{4}} \tag{1}$$

This equation is applicable only if the cross-section of the I beam is symmetrical about both principal axes. For an I beam with flanges of unequal widths, the problem must be treated in a somewhat different manner.

Consider a beam of the cross-section shown in Fig. 1(*a*), subjected to pure bending as indicated. The problem is to find the expression for the critical value of the bending moment at which the beam will buckle laterally—assuming elastic action.

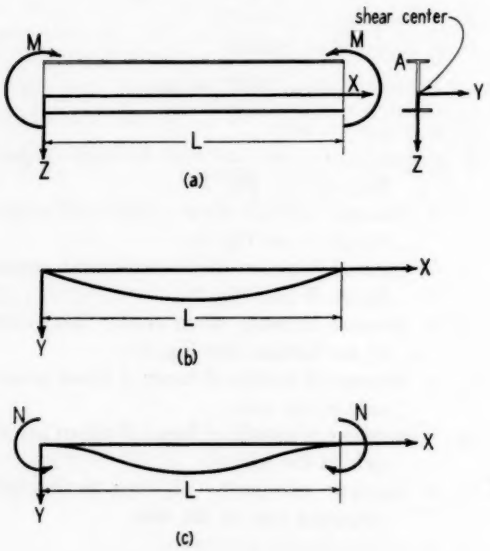

FIG. 1.

Since lateral buckling involves twisting of the beam, it will be necessary to first locate the center of twist or shear center of the section. From the symmetry of the section about a center line in the web, it is evident that the shear center must lie somewhere along this center line. If a length of the beam were supported on a simple span, with the web horizontal, and loaded with a concentrated load applied to the center line of the web at such a distance b from flange B (and a from flange A) that both flanges would deflect alike, there would be no rotation of the section (see Fig. 2). The point at which this load is applied is by definition the shear center of the section. From the consideration that both flanges deflect alike and if the flanges are relatively thin and the bending resistance of the web is neglected, it follows that

$$a/I_B = b/I_A \tag{2}$$

The shear center will lie between the wider flange and the centroid of the section.

Case I: Consider first the case represented by Fig. 1(*b*), with no lateral bending restraint at the extremities of the unsupported length. Taking the axes disposed as indicated in Fig. 1(*a*), the differential equations of equilibrium can be written

$$EI_Z(d^2y/dx^2) = -\theta M \tag{3}$$

$$GJ(d\theta/dx) - E(I_Aa^2 + I_Bb^2)(d^3\theta/dx^3) = M(d/dx)(y + 2e\theta) \tag{4}$$

The difference between these equations and those for a symmetrical I beam, as given by Timoshenko,[2] lies in the expression for the resistance to twisting offered by the flanges, and in the value for the twisting moment. Twisting will occur about the shear center, and since the resistance to twist offered by the two

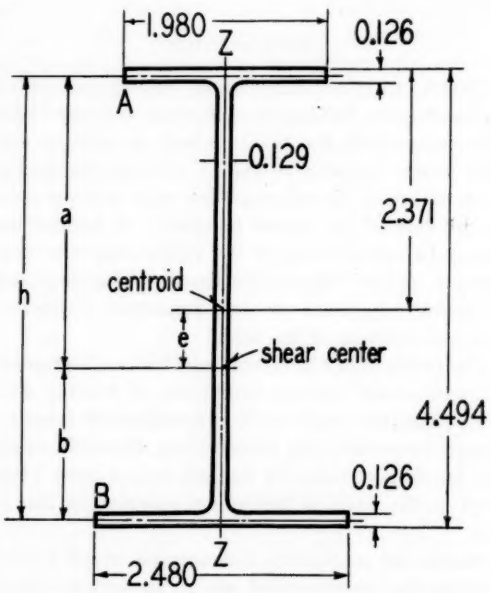

$I_Z = 0.2424$ in.^{4}
$I_A = 0.0815$ in.^{4}
$I_B = 0.1602$ in.^{4}
$J = 0.00619$ in.^{4}
$h = 4.368$ in.
$e = 0.587$ in.

(All dimensions in inches)

FIG. 2.

flanges will be different they must be considered individually. This resistance to twisting offered by the flanges is embodied in the second term of Eq. (4). The expression for the twisting moment is an approximation. It is applicable for unsymmetrical I sections of the sort dealt with in this paper, in which the areas of the two flanges do not differ greatly. The two flanges of an I beam may have the same area, and yet their lateral stiffnesses might be quite different.

Differentiating Eq. (4) and substituting for d^2y/dx^2 its values from Eq. (3) result in the differential equation

$$(d^2\theta/dx^2)(GJ - 2Me) - (d^4\theta/dx^4)E(I_Aa^2 + I_Bb^2) = -(\theta M^2/EI_Z)$$

or, rearranging terms

$$\frac{d^4\theta}{dx^4} - \frac{GJ - 2Me}{E(I_Aa^2 + I_Bb^2)}\frac{d^2\theta}{dx^2} - \frac{M^2}{EI_ZE(I_Aa^2 + I_Bb^2)}\theta = 0 \tag{5}$$

The solution for this fourth order differential equation, with constants determined from the boundary conditions for Case I [Fig. 1(*b*)], *i.e.*, $\theta = 0$, $d^2\theta/dx^2 = 0$ for $x = 0$ and $x = L$, results in the trigonometric equation

$$\sin L\sqrt{-\frac{1}{2g^2} + \sqrt{\frac{1}{4g^4} + \frac{1}{d^4}}} = 0 \tag{6}$$

where

$$1/g^2 = (GJ - 2Me)/E(I_Aa^2 + I_Bb^2) \tag{7}$$

and

$$1/d^4 = M^2/EI_ZE(I_Aa^2 + I_Bb^2) \tag{8}$$

Using the smallest non-trivial root of Eq. (6) yields the equation

$$L\sqrt{-\frac{1}{2g^2} + \sqrt{\frac{1}{4g^4} + \frac{1}{d^4}}} = \pi \tag{9}$$

which, when expanded, can be written

$$1/d^4 = (\pi^4/L^4) + (\pi^2/L^2g^2)$$

Introducing the notation of Eqs. (7) and (8), and collecting terms,

$$M_{cr}^2 + 2(\pi^2/L^2)EI_Zem_{cr} - (\pi^2/L^2)EI_Z \times [GJ + (\pi^2/L^2)E(I_Aa^2 + I_Bb^2)] = 0 \tag{10}$$

which, solved for M_{cr}, gives

$$M_{cr} = \frac{\pi^2EI_Z}{L^2}\left[\sqrt{\frac{L^2}{\pi^2}\frac{GJ}{EI_Z} + \frac{I_Aa^2 + I_Bb^2}{I_Z} + e^2} - e\right] \tag{11}$$

Case II: Next consider the case represented in Fig. 1(*c*), in which the ends of the unsupported length are laterally restrained—*i.e.*, the slope of the lateral-deflection curve remains zero at $x = 0$ and $x = L$. To maintain this configuration, there must be a lateral restraining moment, N, at the ends of the unsupported length.

In determining the critical bending moment for this case, the principles of the "energy" method will be employed. Assume that the loaded beam is given a small lateral deflection, y, with a corresponding twist, θ, and consider the energy of the system compatible with this displacement. When the additional work done by the external moment, M, due to this displacement is just equal to the combined potential energies of twisting and bending with the beam in the deflected position, the beam is in a condition of neutral stability. The corresponding value for M is the critical bending moment for the beam.

Let

U_T = energy of twisting
U_B = energy of bending
U_M = additional work done by the external moment, M, due to the lateral displacement;

then

$$U_M = U_T + U_B \tag{12}$$

It will be convenient to consider the bending of the flanges, due to twisting, in the same equation with the lateral bending of the beam.

$$U_B = EI_A\int_0^{L/2}[(d^2/dx^2)(y + a\theta)]^2dx + EI_B\int_0^{L/2}[(d^2/dx^2)(y - b\theta)]^2dx \tag{13}$$

The lateral bending energy of the web, which is comparatively very small, has been neglected.

The energy of twisting will be

$$U_T = GJ\int_0^{L/2}(d\theta/dx)^2dx \tag{14}$$

The additional work done by the external moment can be expressed

$$U_M = 2M\int_0^{L/2}(d\theta/dx)(d/dx)(y + e\theta)dx$$

or

$$U_M = 2M\int_0^{L/2}[(d\theta/dx)(dy/dx) + e(d\theta/dx)^2]dx \tag{15}$$

The differential equation of lateral bending is

$$EI_Z(d^2y/dx^2) = -M\theta + N \tag{16}$$

Assume for θ the expression

$$\theta = A[1 - \cos(2\pi x/L)] \tag{17}$$

which satisfies the boundary conditions.

From Eqs. (16) and (17)

$$dy/dx = (1/EI_Z)\int \{N - MA\,[1 - \cos(2\pi x/L)]\}\,dx$$

or

$$dy/dx = (1/EI_Z)\,\{Nx - MA[x - (L/2\pi)\sin(2\pi x/L)]\} + C \quad (18)$$

From the conditions

$dy/dx = 0$ when $x = 0$ and when $x = L/2$,

$C = 0$ and $N = MA$

Then

$$dy/dx = (MA/EI_Z)(L/2\pi)\sin(2\pi x/L) \quad (19)$$

Substituting in Eq. (12) the values from Eqs. (13), (14) and (15), and in these latter equations the values for the derivatives determined from Eqs. (17) and (19), the following equation may be obtained.

$$2MA^2\left(\frac{M}{EI_Z} + e\,\frac{4\pi^2}{L^2}\right)\int_0^{L/2}\sin^2\left(\frac{2\pi x}{L}\right)dx = GJ\,\frac{A^2 4\pi^2}{L^2}\times \int_0^{L/2}\sin^2\left(\frac{2\pi x}{L}\right)dx + A^2\left[EI_A\left(\frac{M}{EI_Z} + a\,\frac{4\pi^2}{L^2}\right)^2 + EI_B\left(\frac{M}{EI_Z} - b\,\frac{4\pi^2}{L^2}\right)^2\right]\int_0^{L/2}\cos^2\left(\frac{2\pi x}{L}\right)dx \quad (20)$$

Since

$$\int_0^{L/2}\sin^2(2\pi x/L)dx = \int_0^{L/2}\cos^2(2\pi x/L)dx,$$

$$2M\left(\frac{M}{EI_Z} + e\,\frac{4\pi^2}{L^2}\right) = GJ\,\frac{4\pi^2}{L^2} + EI_A\left(\frac{M}{EI_Z} + a\,\frac{4\pi^2}{L^2}\right)^2 + EI_B\left(\frac{M}{EI_Z} - b\,\frac{4\pi^2}{L^2}\right)^2$$

Collecting terms and simplifying by introducing the relations

$$I_Z = I_A + I_B$$

and

$$a/b = I_B/I_A \text{ [from Eq. (2)]}$$

results in the equation

$$(M^2/EI_Z) + M(8\pi^2/L^2)e - (4\pi^4/L^2)\times [GJ + (4\pi^2/L^2)E(a^2I_A + b^2I_B)] = 0 \quad (21)$$

Solving this equation for M and simplifying, the expression for the critical bending moment is obtained.

$$M_{cr} = \frac{4\pi^2 EI_Z}{L^2}\left[\sqrt{\frac{L^2GJ}{4\pi^2EI_Z} + \frac{I_Aa^2 + I_Bb^2}{I_Z} + e^2} - e\right] \quad (22)$$

A general similarity may be noted between the solutions for the critical moments for the two cases [Eqs. (11) and (22)]. If the coefficient, n, is introduced, and defined in such a way that for Case I, $n = 1$ and for Case II, $n = 2$, the general expression for the critical bending moment may be written as follows:

$$M_{cr} = \frac{n^2\pi^2 EI_Z}{L^2}\left[\sqrt{\frac{L^2GJ}{n^2\pi^2EI_Z} + \frac{I_Aa^2 + I_Bb^2}{I_Z} + e^2} - e\right] \quad (23)$$

This equation can be further simplified by using the relationship

$$I_A + I_B = I_Z$$

and also substituting values for a and b derived from Eq. (2) and the equation

$$a + b = h$$

$$M_{cr} = \frac{n^2\pi^2 EI_Z}{L^2}\left[\sqrt{\frac{L^2GJ}{n^2\pi^2EI_Z} + \frac{I_AI_B}{I_Z^2}h^2 + e^2} - e\right] \quad (24)$$

In this treatment it has been assumed that the narrow flange of the beam was in compression. The solution holds equally well if the beam is inverted. In this case, the sign of e would be negative. The sign of the term e can be determined from the following rule:

If the centroid of the Section lies between the shear center and the compression flange, the sign of e is positive.

It is interesting to note that Eq. (24) reduces to the expression for the critical moment for a symmetrical I beam subjected to pure bending (Eq. 1). This reduction involves the following relations:

$$a = b = h/2$$

$$I_A = I_B = I_Z/2$$

$$e = 0$$

Description and Results of Tests

In making tests to check the analytical solution of a problem, it is frequently difficult to reproduce exactly the conditions assumed in the theoretical treatment. In this particular case, difficulty was anticipated in securing definitely known conditions of restraint at the ends of the unsupported lengths of the beams. It was thought that end conditions representing complete lateral restraint ($n = 2$) could probably be more closely approached and more simply obtained than could end conditions representing lateral support without restraint ($n = 1$).

The beams tested were of a high strength aluminum alloy (Alcoa 17S-T) and had a cross-section of the form of an "I" with flanges of unequal widths (see Fig. 2). Tensile and compressive tests on specimens of the ma-

terial indicated the following average mechanical properties:

Tensile strength	59,000 lbs./in.^{2}
Tensile yield strength (0.2 per cent set)	42,000 lbs./in.^{2}
Compressive yield strength (0.2 per cent set)	38,000 lbs./in.^{2}
Proportional limit	25,000 lbs./in.^{2}

This material has a modulus of elasticity (E) of about 10,300,000 lbs./in.^{2}, and a Poisson's ratio (μ) of 1/3. Average measured dimensions of the cross-section of the beams are given in Fig. 2. Various properties of the section are also tabulated on this figure. The section factor for torsion (J) was determined as the sum of the section factors for three narrow rectangles, representing the two flanges and the web. The portions of the section common to both flange and web were considered in both the flange and web rectangles.

The beams were tested in pairs in order to secure a stable setup. The ends of the two beams were bolted in end restraining frames which were composed of steel plates and angles. Details of these end connections, as well as the manner in which the beams were supported and the load applied, can be seen in Fig. 3.

FIG. 3. Test setup for studying the lateral buckling of unsymmetrical I beams.

The laterally unsupported length of each beam, which was the distance between the points of application of the load, was subjected to pure bending. Strain measurements made on the flanges of both beams, with Huggenberger Tensometers, indicated that the applied load was equally distributed between the two beams.

TABLE 1

RESULTS OF TESTS

Test No.	Laterally Unsupported Length, In.	Maximum Bending Moment (M), In.-Lbs.	Corresponding Stress (S),‡ Lbs. per Sq.In. Narrow Flange	Wide Flange
1*	96	20,100	13,400	12,000
2†	96	31,830	21,300	19,000
3*	72	30,900	20,600	18,500
4†	72	41,850	28,000	25,100

* Narrow flange in compression.

† Wide flange in compression.

‡ Calculated from the relation that stress equals moment divided by section modulus.

Four tests were made, involving two laterally unsupported lengths, 96 in. and 72 in. For each unsupported length, one test was made with the narrow flanges in compression and one with the wide flanges in compression. Failure in all tests occurred by sudden lateral buckling of the beams, which was accompanied by a falling off of the load. The maximum load could therefore be considered as defining the critical buckling strength of the beams. The critical bending moments for each beam, determined from the maximum loads in the four tests, are given in Table 1, together with the corresponding stresses in the flanges.

CORRELATION BETWEEN ANALYTICAL AND EXPERIMENTAL RESULTS

A comparison between the test results and critical bending moments calculated according to Eq. (24) is shown in Table 2. In calculating these values, it has been assumed that the ends of the beams were completely restrained in a lateral direction ($n = 2$). While this is the condition which it was attempted to reproduce in the tests, it was not expected that complete fixity would be obtained. As the values in Table 2 indicate, the test results give values for critical bending moment smaller than the corresponding calculated values. Only in the case of Test No. 4, however, is the difference very great and it can be seen from Table 1 that in this test, stresses above the proportional limit of the material were encountered before buckling of the

TABLE 2

Comparison Between Calculated and Experimentally Determined Values of Critical Bending Moment

Test No.	Laterally Unsupported Length, In.	Critical Bending Moment, In.-Lb. Calculated*	Experimentally Determined	Ratio of Experimentally Determined Bending Moment to Calculated Bending Moment	End Fixity Indicated by Test Results (n Value)
1	96	21,670	20,100	0.93	1.89
2	96	34,230	31,830	0.93	1.93
3	72	34,820	30,900	0.89	1.85
4	72	57,170	41,850	0.73	...

* Calculated according to Eq. (24) using $n = 2$.

beams occurred. In such a case the resistance to lateral buckling is decreased by the plastic action and the beam will buckle under a bending moment smaller than that calculated on the assumption of elastic action.

Assuming that the difference between calculated and measured values of critical bending moment for Tests 1, 2, and 3 reflects a lack of complete lateral restraint at the ends, the degree of restraint obtaining in each test can be determined by substituting the experimentally determined value for critical bending moment in Eq. (24) and solving for the coefficient n. Values for n thus obtained are given in the last column of Table 2. The degree of end restraint is indicated by these coefficients. The values show that the restraint was more nearly complete for the greater unsupported length. These results are consistent with results obtained in a similar investigation involving symmetrical I beams.[3] On the basis of this experience, and in view of the consistent difference between calculated and measured critical bending moments for Tests 1 and 2, the test results can be considered as being substantially in agreement with the analytical solution.

References

[1] Timoshenko, S., *Sur la stabilité des systèmes élastiques*, Annales des Ponts et Chaussées, 9th Series, Paris, 1913.

[2] Timoshenko, S., *Theory of Elastic Stability*, pages 256–279, McGraw-Hill Book Company, New York, 1936.

[3] Dumont, C., and Hill, H. N., *The Lateral Stability of Equal-Flanged Aluminum-alloy I-Beams Subjected to Pure Bending*, N.A.C.A. Technical Note No. 770, August, 1940.

[4] *Structural Aluminum Handbook*, page 48, Aluminum Company of America, Pittsburgh, Pa., 1938.

[5] Moisseiff, Leon S., *Design Specifications for Bridges and Structures of Aluminum Alloy 27S-T*, pages 2–3 and 59–66, Aluminum Company of America, Pittsburgh, Pa., 1940.

Letter to the Editor

February 12, 1942

Dear Sir:

I should like to submit the following discussion of the paper *Determination of Strain Distribution by the Photo-Grid Process* by Given A. Brewer and Robert B. Glassco, appearing in the November, 1941, issue of the Journal.

The authors are to be commended on their work in the application of rational methods to industrial problems. A considerable amount of work of a more strictly research nature has been done on the true stress and true strain properties of materials, and it is gratifying to see this work applied to the problems of industry.

The authors state that a survey of the existing literature reveals that the problem of local strain distribution has received little attention. The appended brief list of references touches on most of the phases of the work which have been studied to date. Reference 4 in particular contains a useful bibliography.

The photo-grid process should prove to be a useful tool for both pure and applied research in materials. As the authors point out, the method makes it possible to determine strains over very small gage lengths. The same is true of the scribing methods which have been in use for some time, although the photo-grid method is probably quicker and cheaper. However, each method is restricted to an average strain over a finite gage length. This method is sufficiently accurate over most of the length of the specimen but it leads to an appreciable error in the region near the fracture, where the strain gradient is large. In this region the strain in an infinitesimal gage length must be used. This strain has been shown[1] to be $\epsilon = \log_e (L/L_0) = \log_e (A_0/A)$, where L_0, L, A_0, and A are the initial and final values of the infinitesimal gage length and the cross-section in question. The strain at the fracture section, which the authors refer to as the "ultimate strain," is the true strain ϵ above with A_0 and A taken at the fracture section. If the initial and final areas have been recorded, it will be possible to complete the authors' Figs. 5 and 6.

Studies of strain distribution in uniaxial specimens of several materials have been made.[2, 4] The results obtained were curves of the same general form as Figs. 5 and 6. A comparison was made in these tests between the true strain ϵ and the customary arbitrary strain $\epsilon_0 = \Delta L_0/L_0$. The authors did not state whether their data were presented as ϵ or ϵ_0. For small strains the difference is negligible, but for large strains the difference can be large. It would be interesting to see some of the authors' two-dimensional strain distributions.

It might be of interest to point out a fundamental difference between the method of the authors and that used by MacGregor in the work referred to above. The authors obtain a distribution of surface strains along the specimen, but their method gives no information as to the state of strain in the interior of the specimen. MacGregor, on the other hand, obtains a distribution of average strains over the cross-section but his method does not give the surface strains directly. A study of true strain distribution using both methods should yield some information of value.

References

[1] MacGregor, C. W., *Relations between Stress and Reduction in Area for Tensile Tests of Metals*, Technical Publication No. 805, Metals Technology, April, 1937.

[2] MacGregor, C. W., *Differential Area Relations in the Plastic State for Uniaxial Stress*, Stephen Timoshenko Sixtieth Anniversary Volume, Macmillan Co., New York, N. Y., 1939.

[3] MacGregor, C. W., *A Two-Load Method of Determining the Average True Stress-Strain Curve in Tension*, Journal of Applied Mechanics, Vol. 6, No. 4, pages A156–A158, December, 1939.

[4] MacGregor, C. W., *The Tension Test*, Proceedings, Amer. Soc. Test. Mat., Vol. 40, pages 508–534, 1940.

[5] de Forest, A. V., MacGregor, C. W., and Anderson, A. R., *Rapid Tension Tests Using the Two-Load Method*, Technical Publication No. 1393, Metals Technology, December, 1941.

[6] Christie, R. E., unpublished research on the two-load method applied to rubber bars in tension, carried out at M.I.T., 1940.

[7] Welch, L. E., unpublished M.S. thesis (M.I.T.) on the two-load method applied to steel bars at elevated temperatures, 1941.

[8] Mehringer, F. J., unpublished B.S. thesis (M.I.T.) on the two-load method applied to rectangular bars and flat sheets in tension, 1941.

W. Kenneth Bodger
Massachusetts Institute of Technology

An Improved Longitudinal Stability Calculation

H. P. LIEPMANN*
University of Cincinnati

ABSTRACT

The conventional method of calculating static longitudinal stability is improved by taking into account the moment of the fuselage in addition to the wing and tail moments about the center of gravity of an airplane. The general equation for the fuselage moment, which is always unstable or stalling, is derived and presented in terms of the dynamic pressure, the angle of attack and two constants which depend on the shape of the fuselage only. These constants are explained theoretically and approximate values for them are given. These approximations lead to a simplified equation for the fuselage moment which is correct up to an angle of attack of about 12°, as shown by comparison with existing experimental results. It is also pointed out, that in calculating the fuselage moment for a stability investigation of an airplane, the downwash induced by the wing should be taken into consideration. A static stability calculation is carried through for an airplane for which the total moment about its center of gravity is known from test results. A comparison of theoretical and experimental values shows that the improved method is in much better agreement with tests than the conventional method of stability calculation.

INTRODUCTION

THE STANDARD investigation of static longitudinal stability takes into account only the moments of the wing and tail about the center of gravity of an airplane. The moments caused by the propeller thrust and drag forces of the fuselage, landing gear, engine nacelles, etc., are so small compared with those of the wing and tail that they are neglected. It has been customary also to neglect the pitching moment of the fuselage, which actually is not negligible compared with the wing and tail moment. The moment of the fuselage can best be calculated by considering the fuselage as a solid moving in a fluid, specifically as an airship. Airship theory shows that there exists an unstable moment, tending to increase the angle of attack. This moment can be of considerable magnitude even though the associated forces are negligibly small, and must be accounted for as required in the Civil Air Regulations, Part 04.2210. The numerical calculation of this moment is based upon a few concepts of airship theory combined with the general momentum theory of moving solids, and is fairly accurate for small angles of attack, say up to 12°. The equation for this pitching moment and its application to a stability calculation will be presented in the following paper.

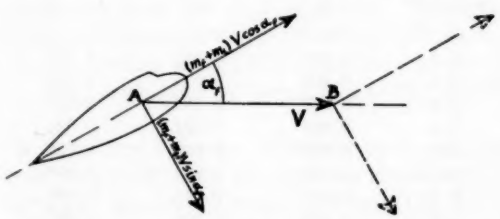

FIG. 1. Momentum components of fuselage and apparent mass.

Received December 16, 1941.

* Instructor in Aeronautical Engineering.

THE PITCHING MOMENT OF A FUSELAGE

The motion of a solid body affects the surrounding air and imparts motion to it. This phenomenon is very pronounced in the immediate neighborhood of the body but gradually decreases with increasing distance from the body. The total mass of air thus affected to a varying amount can be, for the purpose of simple calculation, represented by a fictitious mass of air affected uniformly and moving with the same velocity as the body. This fictitious mass is generally called "apparent mass" and has to be added to the actual mass of the body if the application of the general equations of motion shall give correct results. The most important property of this apparent mass is that it may not be the same for motion in different directions.[1]

Consider a fuselage of mass m_f, moving under an angle of attack α_f with uniform horizontal velocity V feet per second (Fig. 1). Let m_l and m_t be the apparent masses of air associated with the components of motion parallel and perpendicular, respectively, to the longitudinal axis of the fuselage. Then, since momentum equals mass times velocity, there are two components of momentum associated with the fuselage and its apparent mass (Fig. 1).

$$(m_f + m_l)V \cos \alpha_f \text{ and } (m_f + m_t)V \sin \alpha_f$$

Let the horizontal distance AB (Fig. 1) represent the path of the fuselage during a unit time interval. The rate of change of moment of momentum is equal to the moment of the forces exerted by the fuselage on the surrounding air, by virtue of the fundamental laws of motion.

If the velocity V and angle of attack α_f are constant, the moment of momentum about point A changes uniformly from zero to

$$(m_f + m_l)V \sin \alpha_f V \cos \alpha_f - (m_f + m_t)V \cos \alpha_f V \sin \alpha_f = [(m_t - m_l)V^2 \sin (2\alpha_f)]/2$$

with stalling moments taken as positive. Similarly the moment about B changes from $(m_t - m_l)V^2 \sin (2\alpha_f)/2$ to zero. Hence the change of moment of momentum is independent of the point about which the moment is taken, and the total change (and also the rate of change) is equal to

$$[(m_t - m_l)V^2 \sin (2\alpha_f)]/2$$

The moment acting on the fuselage itself is the negative of this, or

$$M = [(m_t - m_l)V^2 \sin (2\alpha_f)]/2 \quad (1)$$

taken positive when stalling.

The only quantities not known up to this point are the two apparent mass components m_l and m_t, associated with the longitudinal and transverse components of motion, respectively. As will be seen later m_t is always greater than m_l. Hence, M, as given in Eq. (1), is a stalling, or unstable, moment at positive angles of attack.

Calculation of Apparent Mass

It is common practice to define, instead of the apparent mass itself, its volume as a certain percentage of the volume of the moving body. Thus, if Q is the volume of the fuselage, and Q_{app} is the apparent mass volume,

$$Q_{app} = kQ \quad (2)$$

where the factor k depends on the shape and the direction of motion of the body. For the two components of motion under consideration

$$Q_l = k_l Q, \; Q_t = k_t Q \quad (3)$$

where Q_l and Q_t are the volumes of the apparent masses for longitudinal and transverse motion of the fuselage, respectively. The corresponding apparent mass components are

$$m_l = \rho k_l Q, \; m_t = \rho k_t Q \quad (4)$$

where ρ is the mass density of air and k_l and k_t dimensionless coefficients.

The two coefficients, k_l and k_t, are functions of the fuselage shape only. They can be calculated mathematically for a few solids of revolutions, for instance, ellipsoids of revolution, which, unfortunately, do not closely resemble conventional fuselage shapes. Table 1 gives values of k_l and k_t, as well as $(k_t - k_l)$, for ellipsoids of revolution of different "fineness ration" n, which is defined as total length L divided by the maximum cross-sectional diameter D. Methods for determining the coefficients k_l and k_t for airship shapes other than an ellipsoid are given in reference 3.

The theoretical calculation of k_l and k_t for any actual fuselage shape would probably offer tremendous difficulties and may even be impossible. However, representative values of k_l and k_t can be obtained from tests on standard and predominant fuselage shapes.

It is intended to conduct such tests in the near future and present the results in another paper. The experimental method to be used is briefly as follows. The fuselage model under consideration is suspended as a physical or torsional pendulum in longitudinal and transverse position. Measuring the period of the pendulum in each position and comparing it with the period of a theoretical pendulum will give the apparent mass components and ultimately the coefficients k_l and k_t. These tests can be made in any fluid which will permit accurate measurement of the period.

As long as actual values of k_l and k_t for fuselage shapes are lacking, the quantity $(k_t - k_l)$ can be taken as approximately 0.6. This value has been derived from moment measurements of a few fuselages in wind tunnels, and leads, as will be shown later, to a satisfactory approximation of Eq. (1). Using $(k_t - k_l) = 0.6$, together with Eq. (4), Eq. (1) reduces to

$$M = 0.6qQ \sin 2\alpha_f \quad (5)$$

where $q = \rho V^2/2$.

Approximate Equation for the Fuselage Moment

The introduction of an average value for the apparent mass coefficients justifies additional approximations leading to a very simple expression for the fuselage moment.

First, the fuselage volume Q is a quantity not generally calculated in designing an airplane. Furthermore its calculation is by no means a simple matter. It is therefore recommended to write the fuselage volume as

$$Q = KAL \quad (6)$$

where L is the overall length, A the maximum cross-sectional area of the fuselage and K a numerical constant for each fuselage shape. For ellipsoids for instance, K equals 2/3 and for actual fuselages K lies within 0.6 and 0.7.

Second, the sine of twice the angle of attack α_f can,

Table 1

Apparent Mass Coefficients for Ellipsoids of Revolution

$n = L/D$	k_t	k_l	$(k_t - k_l)$
1	0.5	0.5	0
1.5	0.621	0.305	0.316
2.0	0.702	0.209	0.493
2.5	0.763	0.156	0.607
3.0	0.803	0.122	0.681
4.0	0.860	0.082	0.778
5.0	0.895	0.059	0.836
6.0	0.918	0.045	0.873
7.0	0.933	0.036	0.897
8.0	0.945	0.029	0.916
9.0	0.954	0.024	0.930
10.0	0.960	0.021	0.939
∞	1.000	0	1.000

for all practical purposes, be replaced by twice the angle of attack in radians itself. This simplification naturally limits the range of applicability of the moment equation, Eq. (5), but gives sufficiently accurate values up to angles of attack of 12 to 15°. Beyond this range, the application of Eq. 1, even in its exact form, will not give moment values in agreement with tests. This discrepancy is exhibited in reference 2, where theoretical and experimental moments for airships and other bodies are compared. It is interesting to note[2] the similarity between fuselage moment and lift coefficient of an air-foil as functions of the angle of attack. Both quantities vary lineally with the angle of attack until the angle approaches a critical value corresponding to the stalling or burble point.

Instead of the actual moment itself, it will be convenient to use a non-dimensional coefficient C_f defined by the relation

$$M = C_f q A L \tag{7}$$

The introduction of Eqs. (5) and (6) in Eq. (7) gives

$$C_f = 0.6K \sin 2\alpha_f$$

According to the fuselage under consideration, a particular value for K, defined in Eq. (6), should be chosen. Assuming this value to be 0.64, and replacing $\sin 2\alpha_f$ by $2\alpha_f/57.3$, the moment coefficient becomes in terms of α_f in degrees

$$C_f = 0.0134\alpha_f \tag{8}$$

In Fig. 2 this relation is plotted and compared with test results on five different fuselages. It is seen that Eq. (8) is in good agreement with the test results.

It is unfortunate that no recent tests on fuselage moments have been conducted so that Eq. 8 could be modified, if necessary, to hold true for current fuselage shapes. It is hoped that this missing information will be supplied before long by a series of simple wind tunnel tests.

Application to Longitudinal Stability Calculation

The calculation of static longitudinal stability is concerned with plotting the total moment, or rather the moment coefficient, about the center of gravity of the airplane against the angle of attack. This graph gives information about the required stabilizer setting, elevator deflections and degree of stability of the airplane. It is also used in dynamic stability calculations.

It is customary to neglect moments due to drag and propeller thrust and to let the total moment be the sum of the wing, tail and fuselage moments. It will be convenient to use a moment coefficient referred to the wing area S and the mean aerodynamic chord C of the wing thus,

$$M = C_m q C S \tag{9}$$

The moment coefficient C_m for the total moment can then be written as the sum of the wing, tail and fuselage moment coefficients, all defined according to Eq. (9)

$$C_m = C_{m_w} + C_{m_t} + C_{m_f} \tag{10}$$

The calculation of the wing moment coefficient C_{m_w} and the tail moment coefficient C_{m_t} is well known. The fuselage moment coefficient C_{m_f}, referred to the wing area and chord, is obtained from equation Eqs. (7) and (9), giving

$$C_{m_f} = C_f A L/(SC) \tag{11}$$

Let α_i be the angle between wing chord and fuselage axis. Then,

$$\alpha_f = \alpha - \alpha_i \tag{12}$$

if α_i is taken positive when wing chord and fuselage axis intersect behind the trailing edge.

Eq. (12) does not take into account that the part of the fuselage aft of the wing lies in the downwash.

From elementary wing theory it is known that for a wing with minimum induced drag, which means elliptical planform, the angle of downwash in degrees at the trailing edge is

$$\epsilon = 57.3 C_L/(\pi R) \tag{13}$$

where C_L is the lift coefficient of the wing and R the aspect ratio. At an infinite distance behind the wing

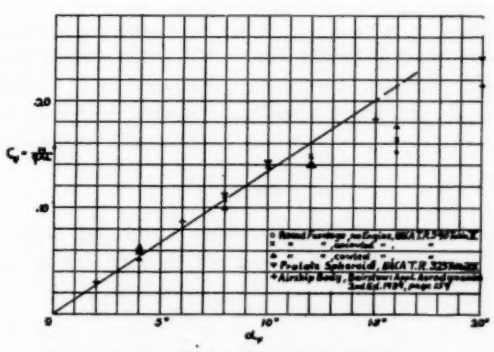

FIG. 2. Fuselage pitching moment coefficient.

the angle of downwash has twice the value given in Eq. (13). For wings with planforms other than elliptical, the downwash angle is slightly greater than that given in Eq. (13). Taking these facts into account, and recalling that Eq. (8) was an approximation also, it seems permissible to assume that the average angle of downwash for the fuselage is

$$\epsilon_f = 1.3(57.3C_L)/(\pi R) = (74.5C_L)/(\pi R) \tag{14}$$

where ϵ_f is taken as positive when the relative wind is deflected downward.

Combining Eqs. (14) and (12), the final fuselage angle of attack becomes

$$\alpha_f = \alpha - \alpha_i - (74.5C_L)/(\pi R) \qquad (15)$$

This value must be used in Eq. (8).

Comparison with Tests

Reference 4 presents wind tunnel tests on airplane models, giving the total moment coefficient. For the fuselage wing combination No. 311, the total moment coefficient has been calculated by the conventional and the improved method advocated in this article. In calculating the tail moment coefficient, the exact angle of downwash at the tail was used according to reference 5. The results are presented in Fig. 3 and show the degree of improvement. Of particular importance is the better agreement in the slope of the moment coefficient curve. It is obvious that the fuselage wing interference cannot be taken care of in this simple calculation. This would account for the discrepancy still remaining between theory and experiment. In all cases, where no complete wind tunnel tests are available, the relatively simple addition of the fuselage moment to the wing and tail moments, gives more accurate results than the conventional method. This is of considerable importance for large and high-speed airplanes, where the stability problem becomes very important.

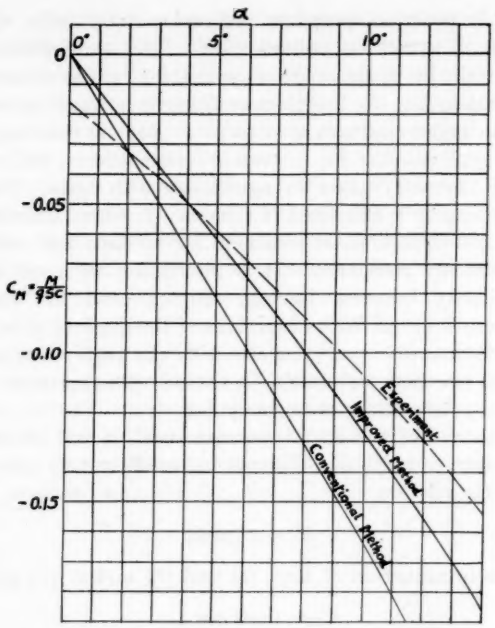

Fig. 3. Comparison of moment coefficient curves.

References

[1] Munk, M. M., *Fundamentals of Fluid Dynamics for Aircraft Designers*, Ronald Press, New York, 1929.

[2] Zahm, A. F., *Flow and Force Equations for a Body Revolving in a Fluid*, N.A.C.A. Technical Report No. 323, 1929.

[3] Upson, R. A., and Klikoff, W. A., *Application of Practical Hydrodynamics to Airship Design*, N.A.C.A. Technical Report No. 405, 1932.

[4] Sherman, A., *Interference of Wing and Fuselage from Tests of Eight Combinations in the N.A.C.A. Variable-Density Tunnel Combinations with Tapered Fillets and Straight-Side Junctures*, N.A.C.A. Technical Note No. 642, 1938.

[5] Silverstein, A., and Katzoff, S., *Design Charts for Predicting Downwash Angles and Wake Characteristics Behind Plain and Flapped Wings*, N.A.C.A. Technical Report No. 648, 1939.

Some Simplified Methods in Airfoil Theory

M. A. BIOT*

California Institute of Technology

Introduction

The use of the acceleration potential in thin airfoil theory was introduced by L. Prandtl.[1,2,6] The method has since been applied by several authors[3,4,5,8] to problems of stationary and non-stationary flow in both compressible and incompressible fluids. A striking feature of this method is that no use has to be made of vortex wakes because the acceleration potential is everywhere continuous in the fluid. Such concepts as the trailing vortices and the induced downwash play no direct part in this theory.

The purpose of the present article is the treatment of two dimensional airfoil theory in an incompressible fluid by the combined use of conformal transformation and the acceleration potential. This method of approach greatly simplifies the solution of certain airfoil problems.

First the reader is introduced to the fundamental properties of the acceleration potential in an incompressible fluid. Then it is shown how the problem of finding the acceleration potential can be solved by conformal representation of the airfoil on a circle and a simple relation is derived between the velocity and the "stream function" corresponding to this potential. The method is next applied to the stationary airfoil with and without flap, and to the determination of the airfoil camber line and thickness function for a given pressure distribution along the chord. The simplicity of the method is especially apparent for the case of the oscillating airfoil which is the subject of the last treatment. For the sake of brevity only translatory oscillations are considered.

Properties of the Acceleration Potential

Newton's law applied to fluid motion leads directly to the equation

$$\rho a = -\text{grad } p \tag{1.1}$$

where ρ = the mass per unit volume, $\bar{a}$ = the acceleration vector, and p = the pressure.

For an incompressible fluid ρ = const., and Eq. (1.1) implies the existence of a scalar function φ such that

$$\begin{aligned} \bar{a} &= \text{grad } \varphi \\ \rho\varphi &= -p\dagger \end{aligned} \tag{1.2}$$

φ is called the *acceleration potential.*

The velocity $\bar{u}$ considered as a vector field function of the coordinates x, y, z and the time t is related to the acceleration by Euler's kinematic equations

$$\bar{a} = (\partial\bar{u}/\partial t) + (\bar{u}.\nabla)\bar{u} \tag{1.3}$$

Assume the velocity field to be composed of a uniform velocity $\overline{U}$ along the x direction and a *small perturbation* $\bar{u}'$.

$$\bar{u} = \overline{U} + \bar{u}' \tag{1.4}$$

Introducing the so-called *linearized theory* which neglects all quantities of higher order in $\bar{u}'$, Eq. (1.3) becomes

$$\bar{a} = (\partial\bar{u}'/\partial t) + U(\partial\bar{u}'/\partial x) \tag{1.5}$$

For an incompressible fluid the velocity $\bar{u}'$ also satisfies the continuity equation

$$\text{div } \bar{u}' = 0 \tag{1.6}$$

Taking the divergence on both sides of Eq. (1.5)

$$\text{div } a = 0 \tag{1.7}$$

hence from (1.2)

$$\nabla^2\varphi = 0 \tag{1.8}$$

The important result is thus obtained that in the linearized theory of an incompressible fluid the acceleration potential satisfies Laplace's equation. If there is a velocity potential ϕ,

$$\bar{u}' = \text{grad } \phi \tag{1.9}$$

and from Eq. (1.5) the following relation is derived between the acceleration and velocity potential.

$$\varphi = (\partial\phi/\partial t) + U(\partial\phi/\partial x) \tag{1.10}$$

In this method of approach flow problems are solved by considering the field of accelerations and using for the acceleration potential solutions of Laplace's equation. The velocity potential and the velocity field may then be derived by integrating Eq. (1.10) with ϕ as an unknown function. The above equations are applicable to thin airfoils where the velocity perturbation $\bar{u}'$ introduced by the airfoil is small compared to the main stream velocity U. It will be shown below

Received October 11, 1941.

* Research Associate in Aeronautics. (On leave of absence from Columbia University.)

† To be absolutely general this equation should contain an additional term which is an arbitrary function of time independent of the coordinates. This term can be omitted for our purpose because $\bar{a}$ and ϕ are taken to vanish at infinite distance in all applications treated in this article.

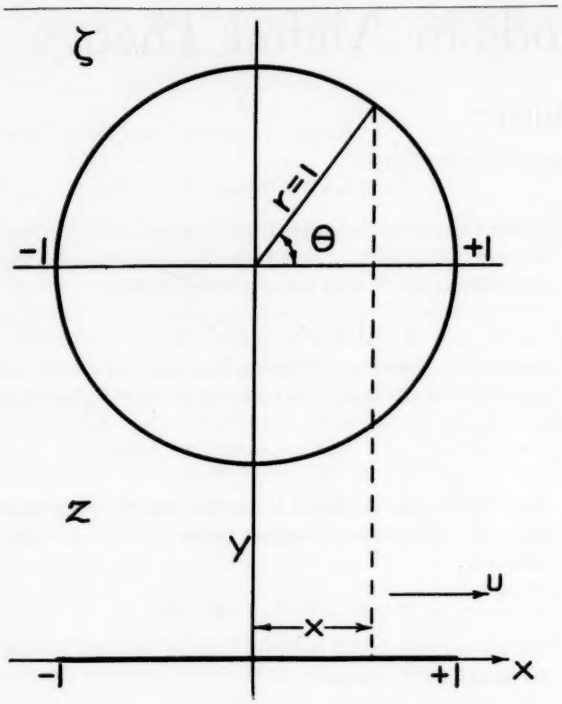

FIG. 1.

how this can be applied in the case of two dimensional airfoil theory.

TWO DIMENSIONAL AIRFOIL THEORY

According to the results derived in the previous paragraph the solution of thin airfoil problems depends on finding a solution of Laplace's equation for the acceleration potential. This potential will be determined by the condition that the acceleration normal to the airfoil has a given value depending on the shape and motion of the airfoil. The case of the airfoil of infinite span will be treated by this method. The flow is then two dimensional. Take x and y to be the coordinates in the plane of flow and the airfoil section to lie approximately along the x axis with the leading edge at $x = -1$ and the trailing edge at $x = +1$. The equation of the airfoil boundary for the general case of a movable or deformable airfoil is

$$y = y(x,t) \tag{2.1}$$

For a thin airfoil, neglecting higher order terms, the coordinate x of a fluid particle moving along the boundary is of the form

$$x = x_0 + Ut \tag{2.2}$$

Hence its velocity normal to the boundary is

$$\dot{y} = U(\partial y/\partial x) + (\partial y/\partial t) \tag{2.3}$$

and its normal acceleration

$$\ddot{y} = U^2(\partial^2 y/\partial x^2) + 2U(\partial^2 y/\partial x \partial t) + (\partial^2 y/\partial t^2) \tag{2.4}$$

Two dimensional potential problems are conveniently handled by conformal transformation. The equation

$$x + iy = z = [\zeta + (1/\zeta)]/2 \tag{2.5}$$

transforms the circle of unit radius in the ζ plane to a straight segment from $x = -1$ to $x = +1$ on the real axis of the z plane (Fig. 1). The point of polar coordinates $r = 1$ and θ on the circle corresponds to the point of coordinate $x = \cos\theta$ on the airfoil. The problem is then to find a complex function

$$f(\zeta) = \varphi + i\psi \tag{2.6}$$

such that the normal derivatives of the acceleration potential φ on the circle satisfy the values derived from the kinematic equation (2.4) for the normal accelerations on the airfoil.

The two functions φ and ψ are conjugate harmonic and satisfy the so-called Cauchy relations

$$\begin{aligned}(\partial\varphi/\partial x) &= (\partial\psi/\partial y)\\ (\partial\varphi/\partial y) &= -(\partial\psi/\partial x)\end{aligned} \tag{2.7}$$

Use is made of these relations for the following reason. The condition that the normal acceleration components satisfy the kinematic boundary condition on the wing does not necessarily imply that the kinematic condition is satisfied for the velocity. Therefore it is necessary to derive the value of the y component of the velocity,

$$v = (\partial\phi/\partial y) \tag{2.8}$$

Taking the y derivative of both sides of Eq. (1.10)

$$(\partial\varphi/\partial y) = (\partial v/\partial t) + U(\partial v/\partial x) \tag{2.9}$$

and from (2.7)

$$-(\partial\psi/\partial x) = (\partial v/\partial t) + U(\partial v/\partial x) \tag{2.10}$$

There are two important cases to consider. For a stationary airfoil the term $(\partial v/\partial t)$ vanishes. In this case, integrating both sides of Eq. (2.10) with respect to x and assuming that both ψ and v are zero at infinity, gives

$$v = -\psi/U \tag{2.11}$$

Hence the simple result that v is proportional to the conjugate function of the acceleration potential.

In the case of non-stationary flow for an airfoil performing harmonic oscillations the functions φ, ψ and v are replaced, respectively, by $\varphi e^{i\omega t}$, $\psi e^{i\omega t}$ and $ve^{i\omega t}$. Eq. (2.10) becomes

$$-(\partial\psi/\partial x) = i\omega v + U(\partial v/\partial x) \tag{2.12}$$

Solving for v as an ordinary linear differential equation and assuming that $v = 0$ at $x = -\infty$ gives

$$v = -(e^{-i\omega x/U}U)\int_{-\infty}^{x} e^{i\omega x/U}(\partial\psi/\partial x)dx \tag{2.13}$$

It must be remarked that the imaginary number i used in connection with harmonic functions of time in Eqs. (2.12) and (2.13) is different from the imaginary number appearing in the complex potential, Eq. (2.6).

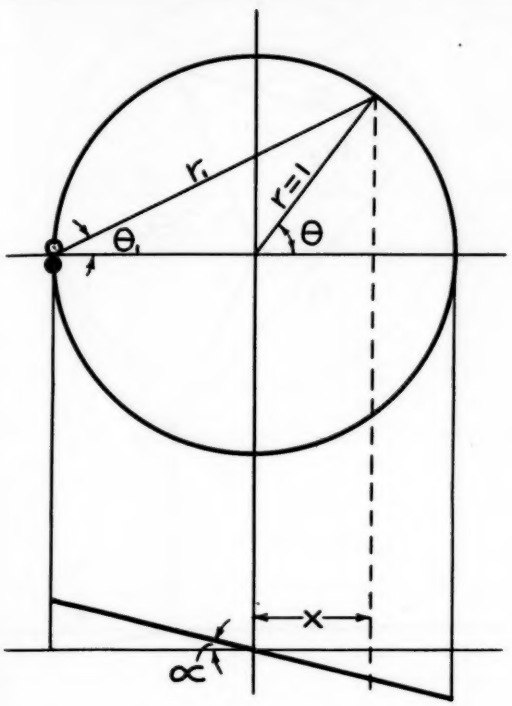

FIG. 2.

Actually different notations should be introduced to distinguish between them. However in the following applications they will not be used simultaneously so that confusion is easily avoided.

The Kutta-Joukowski condition in the classical theory states that the velocity is finite at the trailing edge. An equivalent form of this condition is that there is no pressure discontinuity at the trailing edge. The Kutta-Joukowski condition is therefore taken care of in the present theory by choosing an acceleration potential which is continuous at the trailing edge.

THE STATIONARY AIRFOIL

Symmetric Airfoil

Consider a thin symmetric airfoil at an angle of attack α (Fig. 2). Eq. (2.1) becomes

$$y = -\alpha x \tag{3.1}$$

From Eqs. (2.3) and (2.4)

$$\dot{y} = -\alpha U, \quad \ddot{y} = 0 \tag{3.2}$$

The normal acceleration on the airfoil must be zero; therefore in the z plane the vertical component of the acceleration potential gradient must be zero on the circle. A potential satisfying this condition is that due to a source-sink doublet at the point of coordinate $\zeta = -1$. The conjugate harmonic functions for this case are

$$\begin{aligned} \varphi &= A(\sin \theta_1/r_1) \\ \psi &= A(\cos \theta_1/r_1) \end{aligned} \tag{3.3}$$

where θ_1 and r_1 are the polar coordinates shown in Fig. 2. It is clear that this solution satisfies the Kutta-Joukowski condition that φ is continuous at the trailing edge. On the circle ψ is a constant

$$\psi = A/2 \tag{3.4}$$

The circle is a streamline of the acceleration potential but the constant A which determines the intensity of the doublet must be evaluated by introducing the kinematic condition for the velocity. From Eqs. (2.11), (3.2) and (3.4) at the airfoil

$$v = -\alpha U = -(A/2U) \tag{3.5}$$

Hence

$$A = 2\alpha U^2 \tag{3.6}$$

Hence from Eqs. (1.2) and (3.3) the pressure distribution on the airfoil

$$p = -2\alpha\rho U^2 (\sin \theta_1/r_1) \tag{3.7}$$

The lift distribution l is the pressure difference on both sides; introducing the values $\theta_1 = \theta/2$, $r_1 = 2 \cos(\theta/2)$ gives

$$l = 2\alpha\rho U^2 \tan(\theta/2) \tag{3.8}$$

which is the well known lift distribution on a thin airfoil (Fig. 3). The zero lift at the trailing edge is due to the Kutta-Joukowski condition. The total lift is

$$L = \int_{-1}^{+1} l dx = \int_0^{\pi} l \sin\theta d\theta = 2\pi\alpha\rho U^2 \tag{3.10}$$

The resultant of this lift distribution is located at the quarter chord point.

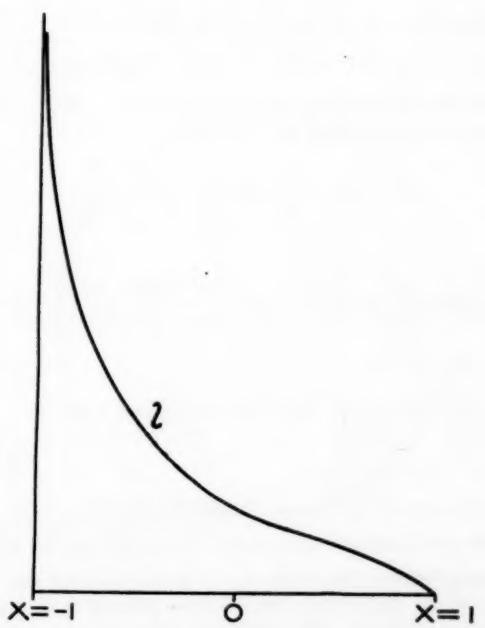

FIG 3

Airfoil with Flap

The case of an airfoil with flap is handled similarly. The same doublet as in the previous case is located at the point corresponding to the leading edge. In addition a source and sink are located on the circle at the points θ_0 and $-\theta_0$, respectively (Fig. 4). These points correspond to a flap hinge of coordinate

$$x = \cos \theta_0$$

The total acceleration potential is

$$\varphi = A \sin \theta_1/r_1 + B \log (r_2/r_3) \tag{3.11}$$

and the corresponding conjugate function is

$$\psi = A \cos \theta_1/r_1 + B\theta_2 \tag{3.12}$$

It is immediately verified that the circle belongs to the streamlines of this source-sink system. The constants A and B determine the strength of these sources and sinks. Their values are fixed by the kinematic condition of the velocity. The y component of the velocity forward of the hinge is obtained from Eqs. (2.11) and (3.12).

$$v = -(A/2U) - (B\theta_0/U) \tag{3.13}$$

This velocity must be zero because the angle of attack of the airfoil is assumed to be zero forward of the hinge, hence the equation

$$-A - 2B\theta_0 = 0 \tag{3.14}$$

Similarly aft of the hinge the vertical velocity is $v = -\beta U$ where β denotes the flap angle, hence the equation

$$-\beta U = -(A/2U) - (B/U)(\theta_0 - \pi)^* \tag{3.15}$$

Solving Eqs. (3.14) and (3.15) for A and B

$$A = 2\beta U^2(\theta_0/\pi) \qquad B = -(\beta U^2/\pi)$$

The lift distribution derived from the value of the acceleration potential Eq. (3.11) is,

$$l = 2\beta\rho U^2\left[\frac{\theta_0}{\pi}\tan\frac{\theta}{2} + \frac{1}{\pi}\log\frac{r_3}{r_2}\right]$$

or

$$l = 2\beta\rho U^2\left[\frac{\theta_0}{\pi}\tan\frac{\theta}{2} + \frac{1}{\pi}\log\left|\frac{\sin {}^1/_2(\theta + \theta_0)}{\sin {}^1/_2(\theta - \theta_0)}\right|\right] \tag{3.16}$$

The total lift is

$$L = \int_{-1}^{+1} l dx = \int_0^{\pi} l \sin\theta d\theta = 2\beta\rho U^2(\theta_0 + \sin\theta_0) \tag{3.17}$$

Airfoil With Given Pressure Distribution

The derivation of the camber line and the thickness function for a given pressure distribution along the airfoil by the use of the acceleration potential is shown for the particular case of an airfoil with uniform pressure.

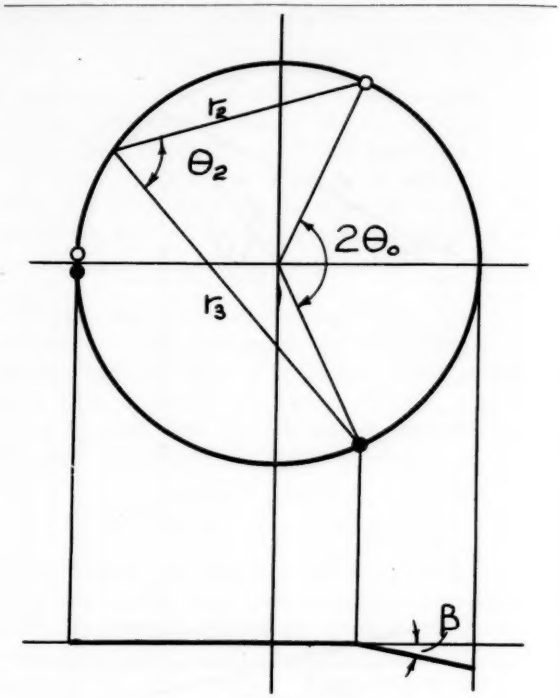

Fig. 4.

Camber Line of Airfoil with Uniform Pressure

The potential due to a pair of equal and opposite vortices at points $+1$ and -1 on the circle (Fig. 5) is

$$\varphi = A(\theta_2 - \theta_1) \tag{4.1}$$

and the conjugate harmonic function

$$\psi = A \log (r_1/r_2) \tag{4.2}$$

On the upper half circle the acceleration potential φ is obviously equal to

$$\varphi = (\pi/2)A \tag{4.3}$$

and on the lower half circle

$$\varphi = -(\pi/2)A \tag{4.4}$$

This gives a uniform lift distribution along the chord.

$$l = \pi\rho A \tag{4.5}$$

The normal velocity is given by Eq. (2.11). Using Eqs. (2.3), (4.2) and (4.5) the following equation is obtained

$$U(dy/dx) = -(l/\pi\rho U)\log (r_1/r_2) \tag{4.6}$$

Substituting the values $r_1^2 = 2(1 + x)$, $r_2^2 = 2(1 - x)$ which are simple to derive geometrically, Eq. (4.6) becomes

$$(dy/dx) = (l/2\pi\rho U^2)[\log (1 - x) - \log (1 + x)] \tag{4.7}$$

* With reference to Fig. 4 it must be kept in mind that the vertex of the angle θ_2 is to be considered as lying in the region outside of the circle. Therefore when passing from the forward to the aft side of the hinge, θ_2 decreases by the amount π.

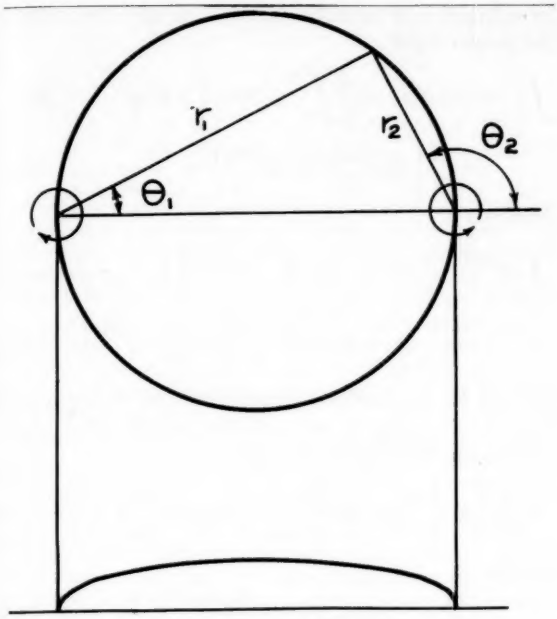

FIG. 5.

Integrating with the condition that $y = 0$ at the leading and the trailing edge the following expression is obtained for the camber line

$$y = \frac{l}{2\pi\rho U^2}\Big[2\log 2 - (1+x)\log(1+x) - (1-x)\log(1-x)\Big] \quad (4,8)$$

This camber line is represented in Fig. 5.

Thickness Function of Airfoil with Uniform Pressure

In a similar way the thickness function for an airfoil with uniform pressure distribution can be found. The harmonic conjugate functions for this case are obtained from two doublets at points -1 and $+1$ as indicated in Fig. 6.

$$\varphi = A[(\cos\theta_1/r_1) - (\cos\theta_2/r_2)]$$
$$\psi = -A[(\sin\theta_1/r_1) - (\sin\theta_2/r_2)] \quad (4.9)$$

The pressure on both sides of the airfoil is uniform and equal to

$$p = -\rho\varphi = -\rho A$$

Proceeding as above leads to the equation

$$U\frac{dy}{dx} = \frac{A}{U}\left[\frac{\sin\theta_1}{r_1} - \frac{\sin\theta_2}{r_2}\right] \quad (4.10)$$

This may be written

$$(dy/dx) = -(p/2\rho U^2)[\tan(\theta/2) - \cot(\theta/2)]$$

or since $dx = -\sin\theta d\theta$

$$dy = (p/\rho U^2)\cos\theta d\theta \quad (4.11)$$

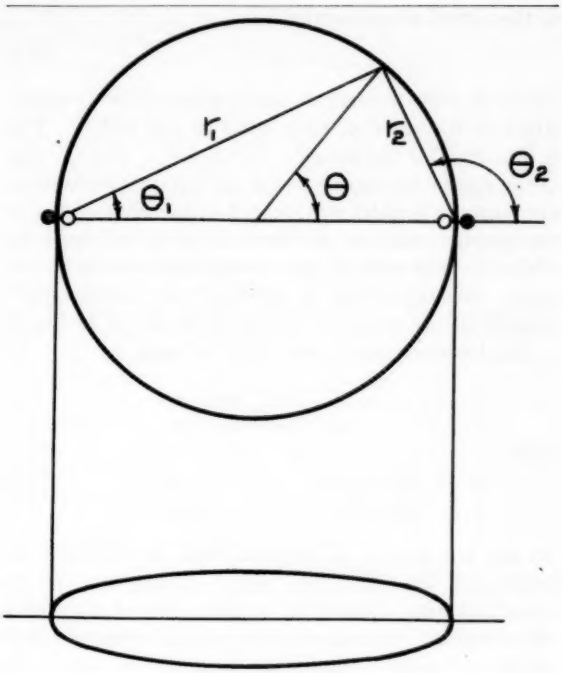

FIG. 6.

The thickness function is found by integration

$$y = -(p/\rho U^2)\sin\theta \quad (4.12)$$

The cross-section given by this thickness function is an ellipse.*

OSCILLATING AIRFOIL

The case of an oscillating airfoil is amenable to a particularly simple treatment by the acceleration potential. As an example the case of vertical translatory oscillations will be considered. The translation

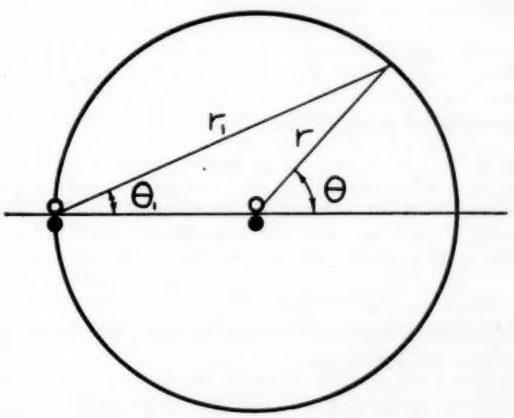

FIG. 7.

* It is clear that the theory breaks down at the leading edge and the trailing edge. This is due to essential limitations of the so-called thin wing theory which is only a first order approximation.

of the airfoil is represented by

$$y = y_0 e^{i\omega t} \tag{5.1}$$

There is now a vertical acceleration $\ddot{y} = -\omega^2 y_0 e^{i\omega}$ which is the same at each point of the airfoil. This is also true for the velocity $\dot{y} = i\omega y_0 e^{i\omega t}$. For the case of the stationary theory in the section on The Stationary Airfoil a doublet was located at the point -1. In the present case an acceleration potential must be added to take care of the vertical acceleration at the wing; this extra term is provided by introducing a doublet at the center of the circle as shown in Fig. 7.

The harmonic conjugate functions are

$$\varphi = \varphi_1 + \varphi_2$$
$$\psi = \psi_1 + \psi_2$$

with

$$\varphi_1 = A(\sin\theta_1/r_1) \quad \varphi_2 = B(\sin\theta/r) \tag{5.2}$$
$$\psi_1 = A(\cos\theta_1/r_1) \quad \psi_2 = B(\cos\theta/r)$$

In the following it is assumed that all functions are multiplied by $e^{i\omega t}$. This factor cancels out of the equations and is therefore dropped out of all expressions below. The acceleration of the wing must be equal to $-\omega^2 y_0$. Hence the value $B = \omega^2 y_0$. The term with B gives rise to the well known apparent mass.

The value of A must be determined by the kinematic condition for the velocity. Using Eq. (2.13) gives for the vertical velocity at a point $x = -1 + \epsilon$ on the airfoil,

$$i\omega y_0 = \frac{-e^{-(i\omega/U)(-1+\epsilon)}}{U} \int_{-\infty}^{-1+\epsilon} e^{i\omega x/U} \left(\frac{\partial\psi_1}{\partial x} + \frac{\partial\psi_2}{\partial x}\right) dx \tag{5.3}$$

This value is independent of the coordinate ϵ on the airfoil so that ϵ can be made infinitely small. There is a singularity at the leading edge and in order to make the expression integrable it is convenient to integrate by parts the term containing $\partial\psi_1/\partial x$. The limiting value for $\epsilon \to 0$ becomes

$$i\omega y_0 = -\frac{\psi_1}{U} + \frac{e^{i\omega/U}}{U} \int_{-\infty}^{-1} e^{i\omega x/U} \left(\frac{i\omega}{U}\psi_1 - \frac{\partial\psi_2}{\partial x}\right) dx \tag{5.4}$$

The value of ψ_1 on the airfoil is

$$\psi_1 = A/2$$

Noting from the conformal transformation (2.5) that

$$r_1 = -x - 1 + \sqrt{x^2 - 1}$$
$$r = -x + \sqrt{x^2 - 1}$$

and substituting $\theta_1 = \theta = \pi$ in Eq. (5.2) it is found that outside the airfoil (for $x < -1$)

$$\psi_1 = -A/(-x - 1 + \sqrt{x^2 - 1})$$
$$\psi_2 = -B/(-x + \sqrt{x^2 - 1})$$

To integrate $\int_{-\infty}^{-1} e^{i\omega x/U}\, \psi_1 dx$ the variable of integration x is replaced by $-x$. In reducing the integrals to the form below care must be exercised to give the radical the proper sign.

$$\int_{-\infty}^{-1} e^{i\omega x/U}\, \psi_1 dx = \frac{A}{2}\int_1^{\infty} e^{-i\omega x/U}\left[1 - \sqrt{\frac{x+1}{x-1}}\right] dx =$$
$$-\frac{A}{2}\left[K_1\left(\frac{i\omega}{U}\right) + K_0\left(\frac{i\omega}{U}\right) + \frac{Ue^{-i\omega/U}}{i\omega}\right] \tag{5.5}$$

Similarly,

$$\int_{-\infty}^{-1} e^{i\omega x/U} \frac{\partial\psi_2}{\partial x} dx = \omega^2 y_0 \int_1^{\infty} e^{-i\omega x/U}\left[1 - \frac{x}{\sqrt{x^2-1}}\right] dx$$
$$= -\omega^2 y_0\left[K_1\left(\frac{i\omega}{U}\right) - \frac{U}{i\omega}e^{-i\omega/U}\right] \tag{5.6}$$

K_0 and K_1 are modified Bessel functions of the second kind.* Eq. (5.4) is an equation for A; after some simple cancellations it becomes

$$-\frac{A}{2U}\left[K_1\left(\frac{i\omega}{U}\right) + K_0\left(\frac{i\omega}{U}\right)\right] - i\omega y_0 K_1\left(\frac{i\omega}{U}\right) = 0 \tag{5.7}$$

Hence

$$A = -2i\omega y_0 U \frac{K_1(i\omega/U)}{K_1(i\omega/U) + K_0(i\omega/U)} \tag{5.8}$$

The lift distribution is obtained from the acceleration potential (5.2),

$$l = \rho A \tan(\theta/2) + 2\rho\omega^2 y \sin\theta \tag{5.9}$$

where A is the complex function of the frequency (5.8).

The second term in Eq. (5.9) represents the apparent mass due to the surrounding fluid. The first term shows that the non-inertia part of the lift distribution is the same as for the stationary case and has its resultant at the quarter chord point.

References

[1] Prandtl, L., *Theorie des Flugzeugtragflügels im zusammendrückbaren Medium*, Luftfahrtforschung, Bd. 13, Nr. 10, pages 313–319, October, 1936.

[2] Prandtl, L., *Beitrag zur Theorie der tragenden Fläche*, Zeit. f. ang. Math. u. Mech., Bd. 16, Heft 6, pages 360–361, December, 1936.

[3] Schlichting, H., *Tragflügeltheorie bei Uberschallgeschwindigkeit*, Luftfahrtforschung, Bd. 13, pages 320–335, 1936.

[4] Kinner, W., *Die kreisförmige Tragfläche auf potentialtheoretischer Grundlage*, Ing. Archiv., Bd. 8, pages 47–80, 1937.

[5] Possio, C., *L'Azione Aerodinamica sul Profilo Oscillante in un Fluido Compressibile a Velocita Iposonora*, L'Aerotecnica, Vol. XVIII, fasc. 4, pages 441–458, April, 1938.

[6] Prandtl, L., *Ueber neuere Arbeiten zur Theorie der tragenden Fläche*, Proceedings International Congress for Applied Mechanics, Cambridge, U.S.A., pages 478–482, 1938. English translation, N.A.C.A. Technical Memorandum, No. 962, December, 1940.

[7] Von Kármán, Th., and Sears, W. R., *Airfoil Theory for Non-Uniform Motion*, Journal of the Aeronautical Sciences, Vol. 5, No. 10, pages 379–390, August, 1938.

[8] Küssner, H. G., *Allgemeine Tragflächentheorie*, Luftfahrtforschung, Bd. 17, pages 370–378, December, 1940. English translation, N.A.C.A. Technical Memorandum, No. 979, June, 1941.

* For an evaluation of the integrals (5.5) and (5.6) see reference (7).

Institute Notes

Midwest Student Sectional Meeting March 21–22 at the University of Notre Dame

A regional meeting of Institute Student Branches in midwestern schools is being held at the University of Notre Dame the week end of March 21–22. Student Branches at University of Cincinnati, University of Detroit, Iowa State College, University of Michigan, University of Minnesota, University of Notre Dame, Tri-State College and Wayne University will participate.

Preliminary arrangements for the meeting were made by Prof. Wilbur C. Nelson, Faculty Adviser of the Student Branch at Iowa State College in cooperation with Prof. F. N. M. Brown of the University of Notre Dame.

Student representatives attending the meeting will register at Notre Dame on Friday evening and Saturday morning. A group breakfast will be held Saturday morning followed by a technical session arranged by Prof. Bradley Jones of the University of Cincinnati, at which student papers will be presented.

Prof. John D. Akerman, University of Minnesota, is in charge of the Saturday Luncheon program at which Lester D. Gardner, Executive Vice-President of the Institute, will be guest speaker. Prof. George H. Tweney, University of Detroit, will lead the afternoon technical session, consisting of talks by faculty members and engineering personnel.

The meeting will conclude with a dinner Saturday evening at which Prof. E. A. Stalker, University of Michigan, will preside. William B. Stout, President of Stout Engineering Laboratories, will be the guest speaker. Awards for student papers will be presented.

News of Institute Members

Allen B. Barton, Technical Member, has been promoted from Engineering Aide to Junior Aeronautical Engineer at the Naval Aircraft Factory.

Don R. Berlin, F.I.Ae.S., has resigned from his position as Chief Engineer of Military Airplanes with the Airplane Division (Buffalo Plants), Curtiss-Wright Corp., to assist in aircraft development and production with General Motors Corp.

Allan E. Bjerke, Technical Member, formerly Assistant Meteorologist, Eastern Air Lines, has joined the Engineering Department of the Airplane Division (Buffalo Plants), Curtiss-Wright Corp.

Lt. (jg) William Bollay, U.S.N.R., A.F.I.Ae.S., is on active duty with the Bureau of Aeronautics, Navy Department, in Washington, having taken leave of absence from the Graduate School of Engineering, Harvard University, where he is Instructor in Applied Mechanics.

Formerly a Junior Aeronautical Engineer with the N.A.C.A. at Langley Field, **Willard B. Boothby,** Technical Member, has joined the Vought-Sikorsky Aircraft Div., United Aircraft Corp., as a Test Pilot.

Chester H. Brown, Jr., Technical Member, formerly a Junior Aeronautical Engineer, Grumman Aircraft Engineering Corp., is now a 2nd Lieutenant in the Coast Artillery.

Harold Caminez, A.F.I.Ae.S., well-known aircraft engine designer, has recently joined the engineering staff of the Lycoming Div., Aviation Mfg. Corp. He was previously Executive Engineer, Air Associates, Inc.

C. C. Moseley, President of Curtiss-Wright Technical Institute and associated schools, has appointed as Assistant to the President **Col. Clifton C. Carter,** A.F.I.Ae.S. Colonel Carter, who was retired recently from active service in the Army, had been Professor of Natural and Experimental Philosophy at the U.S. Military Academy since 1917. He established at West Point its first course in aerodynamics of which he was in charge since 1922. He is the author of the textbook, "Simple Aerodynamics and the Airplane."

Frederick W. Castle, Technical Member, has been granted a leave of absence from his position as Assistant to the President, Sperry Gyroscope Co., to serve with the Army Air Forces.

Dean Thorndike Saville of the College of Engineering, New York University, has announced the appointment of **Charles H. Colvin** as Coordinator of Research for the College. Mr. Colvin, a Fellow and member of the Council of the Institute, is also Director of the Daniel Guggenheim School of Aeronautics at New York University, a post to which he was appointed last summer.

Technical Member **Richard M. Coulston** has been commissioned a 2nd Lieutenant in the Air Corps and assigned to the Experimental Engineering Branch, Materiel Division, at Wright Field as a Structural Engineer. He was formerly Layout Engineer with North American Aviation, Inc.

Don K. Covington, Jr., Technical Member, having received a degree of B.S. in Ae.E. from Parks Air College in December, is now employed as an Engineer with The Glenn L. Martin Co.

M. B. Crawford, M.I.Ae.S., has left United Air Lines, where he was Equipment Engineer, to be Field Service Engineer for Pump Engineering Service Corp. He had previously been an Aeronautical Engineer on the staff of Boeing Aircraft Corp.

Vernon G. Emrich, Technical Member, who was formerly an Engineer with Mercury Aircraft Co., is now Engineering Salvage Supervisor, Airplane Div. (St. Louis Plant), Curtiss-Wright Corp.

Ernest W. Fuller, M.I.Ae.S., has left The Acrotorque Co., where he was Chief Engineer of the Aircraft Division, to go on active duty with the U.S. Navy.

Prof. Ing. Robert Gsell, A.F.I.Ae.S., has been appointed by the Federal Air Office of Switzerland to head its newly created Institute for the Equipment of Aircraft. He was formerly Chief of the Technical Section of the Air Office, which is a bureau of the Swiss Dept. of Post and Railways. Professor Gsell is also on the faculty of the Federal Polytechnical School at Zurich.

Technical Member **Beverly G. Gulick** has been promoted from Junior to Senior Civil Engineer, N.A.C.A., and has been transferred from the Langley Memorial Aeronautical Laboratory to the Aircraft Engine Research Laboratory.

A. M. Hall, M.I.Ae.S., has been appointed Division Manager, Fort Worth Div., Consolidated Aircraft Corp.

A commission as 2nd Lieutenant in the U.S. Army Air Forces, with assignment as Flying Instructor in the Air Corps, was conferred upon **James N. Hall,** Technical Member, in February.

Randolph F. Hall, A.F.I.Ae.S., has joined the staff of Bell Aircraft Corp. as Aeronautical Engineer. He was formerly Chief Engineer, Cunningham-Hall Aircraft Corp.

Lt. Col. Harold E. Hartney, M.I.Ae.S., has been appointed Technical Consultant to Fleetwings, Inc. He is an officer in the Army Air Force Reserve.

F. Leroy Hill, M.I.Ae.S., formerly President of Air Associates, Inc., is now President and General Manager, Aero Screw Company.

Robert R. Houston, Jr., Technical Member, has been transferred from duties as Aircraft Inspector to Engineer Officer, Pan American Airways System.

Robert Insley, F.I.Ae.S., recently Vice-President in charge of Engineering, Menasco Mfg. Co., has joined Kinner Motors, Inc. He has been active in aircraft engine work since 1920. He was in the Power Plant Branch, Materiel Division of the Air Corps at Wright Field for eight years and with United Aircraft

Corp. from 1933 to 1940, when he held the position of Assistant Chief Engineer of the Pratt & Whitney Division.

David E. Irving, Technical Member, is a 1st Lieutenant, Design Development Unit, Aircraft Laboratory of the U.S. Army Air Corps at Wright Field. He was formerly Chief of Structures, Aircraft Div., The Edward G. Budd Mfg. Co.

Dr. John G. Jenkins, M.I.Ae.S., a Lieutenant Commander, U.S.N.R., is on active duty with the Navy Bureau of Aeronautics in Washington. He is Research Director for the Committee on Selection and Training of Aircraft Pilots, National Research Council, and since 1938 had been Professor of Applied Psychology at the University of Maryland.

Formerly a student at Stanford University, **Henry Jessen,** A.F.I.Ae.S., has been appointed Assistant Professor of Aeronautics at the Guggenheim Aeronautical Laboratory there. He has been an aircraft design engineer since 1932, with General Aviation Corp. and then on the staff of Chance Vought Aircraft Div., United Aircraft Corp.

Robert W. King, Technical Member, formerly a Stress Analyst, The Glenn L. Martin Co., has taken a similar position with the Fabrication Div., Dow Chemical Co.

Having completed the required work as Student Engineer with Lockheed Aircraft Corp., **Telfer Kitchen,** Technical Member, has been promoted to Senior Layout Man.

Capt. William H. Klenke, M.I.Ae.S., has resigned as Assistant Sales Manager and Engineering Test Pilot, Vultee Aircraft, Inc., to serve as a pilot officer in the U.S. Marine Corps.

Dipl. Ing. M. Z. Krzywoblocki, M.I.Ae.S., who had been Assistant Supervisor of the Tool Control and Works Methods Dept., Aircraft Div., Canadian Car & Foundry Co. Ltd. for the past several months, is now Assistant Supervisor, Efficiency and Salvage Dept., Noorduyn Aviation Ltd. of Montreal. Before the war, he had been an aircraft designer with P.Z.L., the Polish National Aircraft Co., and in 1940 on the staff of the Amiot company in France.

Dana W. Lee, Associate Mechanical Engineer with the N.A.C.A. at Langley Field, is now Mechanical Engineer, Fuels and Lubricants Section of the Committee's Aircraft Engine Research Laboratory.

Col. Clements McMullen, A.F.I.Ae.S., has recently been promoted from the rank of Major and made Commanding Officer, Third Air Service Area, U.S. Army Air Corps.

William C. McFadden, Technical Member, who was a member of the Lockheed-Cal Tech industrial engineering group in 1940, is a Service Engineer with Pan American-Grace Airways at their maintenance base in Lima, Peru.

Technical Member **Albert E. Mitchell,** who was formerly Aeronautical and Flight Engineer, Cape Aircraft, Inc., is now Chief Draftsman, Experimental Div., AGA Aviation Corp.

Orville E. Mohler, M.I.Ae.S., has left Menasco Mfg. Co., where he was Vice-President in charge of Sales, to go on active duty with the Air Corps at Wright Field.

Donald J. Naumann, M.I.Ae.S., is a Structures Engineer with Vultee Aircraft, Inc.

John D. Peace, Jr., A.F.I.Ae.S., recently in charge of Dayton and Pacific Coast sales for United Aircraft Products, Inc., is now Production Engineer on automatic pilot equipment for Jack & Heintz, Inc. He had previously been Manager of Aeronautical Sales, Sperry Products, Inc., for a number of years.

Recently appointed Chief Aerodynamicist, Aircraft Div., The Edward G. Budd Mfg. Co., is Technical Member **Frank N. Piasecki.** He was formerly on the engineering staff of Platt-LePage Aircraft Co.

Robert M. Pinkerton, M.I.Ae.S., formerly Associate Physicist, Langley Memorial Aeronautical Laboratory, N.A.C.A., is Associate Professor of Aeronautical Engineering, Agricultural & Mechanical College of Texas.

Technical Member **Angelo M. Rocco** has recently been appointed a Junior Aeronautical Engineer at the Naval Aircraft Factory, Philadelphia.

Donald K. Seulke, Technical Member, is now a Draftsman with Vega Airplane Co., having formerly held a similar position with Vought-Sikorsky Aircraft Div., United Aircraft Corp.

H. V. Shebat, A.F.I.Ae.S., has left Wright Aeronautical Corp., where he was Test Engineer and Engineering Pilot, to become an Air Safety Investigator for C.A.A.

John C. Silliman, Technical Member, has been promoted from Assistant Engineer, Structures Dept., Pacific Railway Equipment Co., to the position of Superintendent for the company.

Technical Member **John J. Slattery** has been made Assistant Meteorologist, Transpacific Div., Pan American Airways System.

James Hopkins Smith, Jr., M.I.Ae.S., has been transferred to the staff of Pan American Airways-Africa Ltd. He was previously Assistant Manager, Atlantic Div., Pan American Airways System.

Formerly Station Manager at Knoxville, Tenn., for Pennsylvania-Central Airlines, Technical Member **Joseph W. Stout, Jr.,** has been made Stations Field Supervisor for the company.

John R. Sutton, Technical Member, has left the Engineering Dept. of Lear Aviation, Inc., to join the Electrical Section, Airplane Div. (Columbus Plant), Curtiss-Wright Corp.

Raymond R. Wiese, Technical Member, formerly Western Editor of "Product Engineering" and "The American Machinist," has joined the Engineering Dept. of Fleetwings, Inc.

Richard E. Wildman, Technical Member, has completed the Aviation Cadet training course at Chanute Field and received a commission as 2nd Lieutenant in the Army Air Forces.

Technical Member **John A. Wright,** Stress Analyst, The Glenn L. Martin Co., has been transferred to The Glenn L. Martin-Nebraska Co. as a Structures Engineer.

John S. Wynne, M.I.Ae.S., is conducting a course in aviation law at Southeastern University. From 1933 to 1936 Mr. Wynne was Chief of the Airport Section and then Assistant Director of the Bureau of Air Commerce. Since then he has acted as legal and technical counsel in Washington for airlines, manufacturers and other aviation concerns.

Harold E. Young, Technical Member, recently a student at Parks Air College, is now with Boeing Aircraft Co.

Student Branches

Boeing School of Aeronautics. The following officers of the Student Branch for the first quarter of 1942 were elected: Chairman, R. P. Tuthill; Vice-Chairman, Ralph Horton; Secretary-Treasurer, C. G. David Tharakan.

Casey Jones School of Aeronautics held its most successful social affair of the school year when it sponsored a Senior Dance on February 14. Over fifty couples attended.

Rensselaer Polytechnic Institute. At a meeting on February 12, attended by forty members, Secretary Richard P. Graham presented and led discussion on the illustrated paper, "Seamless Tubing" by J. P. Dods. Chairman George McTigue announced that the papers in competition for the Student Branch Award would be judged at a meeting on March 26. The meeting closed with the showing of the motion picture, "Spark Plugs in Aviation."

Ryan School of Aeronautics. Branch member Philip Balsley presented his paper on "Submerged Engines" at a dinner meeting held on December 5. The lecture dealt with engine installations inside an airplane wing, and was illustrated by pictures of the Northrop "Flying Wing" and an installation of the Lycoming opposed twelve cylinder engine. Joel Whitney, Registrar of

Ryan School, participated in the discussion. Preceding the dinner, Earl D. Prudden, Vice-President of the school, presented diplomas of graduation to Gordon Andrist and Martin Schwartz.

On January 29 the topic of discussion, led by William Rager, was the Branch lecture on "Typical Research Problems of United Air Lines." Two-year engineering diplomas were presented to two alumni guests, Gwynn Crowther and Robert Cerna.

Changes in Membership

The following changes in the membership of the Institute have occurred since the publication of the previous issue of the Journal.

Transferred from Member to Associate Fellow Grade

Donovan, Robert Charles, Project Engineer, Douglas Aircraft Co.

Wood, John Walter, M. Arch.; Airport Consultant, Poor & Wood.

Elected to Member Grade

Haiduck, Andrew Frank, Ae.E.; Chief Engineer, Bellanca Aircraft Corp.

Komarnitsky, Rostislaw S., Supervising Engineer, Armor Plate Div., Breeze Corporations, Inc.

Mayo, William Benson, Consulting Engineer.

Mohyla-Mokrzycki, Gustaw Andrzej, M.Ae.S.; Prof. Ord., Aero Dept., Warsaw Inst. of Technology; Engineer, Aircraft Div., National Steel Car Corp., Ltd., Canada.

Runstad, Harold J., B.S. in C.E.; Structural Test Engineer, Boeing Aircraft Co.

Vandermeer, Will, M.E.; Asst. Chief Engineer, Ryan Aeronautical Co.

Wolf, Robert A., M.S. in Ae.E.; Design Engineer, Bell Aircraft Corp.

Transferred from Technical Member to Member Grade

Coutinho, John De Siqueira, Aero. Engineer, Grumman Aircraft Engineering Corp.

Del Mar, Bruce Eugene, B.S. in M.E.; Cabin Supercharging Engineer, Douglas Aircraft Co.

Walker, Ernest Edward, Chief Landscape Engineer, U.S. Forest Service; Aviation Writer.

Elected to Technical Member Grade

Brooke, Hubert E., B.S. in Ae.E.; Engineer, Consolidated Aircraft Corp.

Griffith, Joseph Fisler, B. A.; Estimator, Selby, Battersby Co.

Hoggard, Hugh Page, Jr., B.S. in M.E.; Asst. Mech. Engineer, Langley Mem. Aero. Lab., N.A.C.A.

O'Brien, Francis X., B.S. in C.E.; Stress Analyst, Grumman Aircraft Engineering Corp.

Thomas, Walter Charles, Assoc. Inspector, Engineering Materials (Aero.), Bureau of Aeronautics, Navy Dept.

Wang, Chao-Hua, M.Sc.

Transferred from Student Member to Technical Member Grade

Anderson, Leon R., B.S. in Ae.E.; Weight Estimator, The Glenn L. Martin Co.

Anderton, David A., Engineer, Grumman Aircraft Engineering Corp.

Beaver, Russel H., Jr., B.S. in Ae.E.; Detail Draftsman, Boeing Aircraft Co.

Beck, Carl A., Aeronautical Service Engineer, Sperry Gyroscope Co.

Brenkert, Ingvald K., Layout-Draftsman, Ford Motor Co.

Carpenter, Dale, B.S. in Ae.E.; Apprentice Engineer, Pan American Airways System.

Carver, George Philander, B.S. in M.E.; Structural Research Engineer, Lockheed Aircraft Corp.

Cerna, Robert F., Engineering Instructor, Ryan School of Aeronautics.

Crane, Leon, B.S. in Ae.E.; 2nd Lieut., U.S. Army Air Corps, Wright Field.

Gaubis, Leonard Louis, Engineer, Grumman Aircraft Engineering Corp.

Golden, James M., B.S. in M.E.; Apprentice Engineer, Vought-Sikorsky Aircraft Div., United Aircraft Corp.

Iszard, Robert F., B.S. in Ae.E.; Testing Engineer, General Electric Co.

Kreitinger, Richard L., B.S. in Ae.E.; Project Engineer, Boeing Aircraft Co.

Letko, William, B.Ae.E.; Jr. Engineer, Langley Mem. Aero. Lab., N.A.C.A.

Maier, Norman M., Engineer, Grumman Aircraft Engineering Corp.

McDonald, J. Wallace, B.Ae.E.; Stress Analyst, Aircraft Div., Edward G. Budd Mfg. Co.

Munro, Robert B., Department Clerk, Grumman Aircraft Engineering Corp.

Muzzey, Clifford Loring, S.B. in Ae.E.; Blade Engineer, Aeroproducts Div., General Motors Corp.

Oehrli, Robert R., Sr. Tool Draftsman, The Glenn L. Martin Co.

Pannell, Robert L., B.S. in M.E.; Jr. Tool Designer, Vega Airplane Co.

Pope, George H., B.S.; Wind Tunnel Asst., Northrop Aircraft Inc.

Randolph, John L., Graduate Student, N. C. State College.

Robinson, Theodore D., B.S. in Ae.E.; Engineer, Grumman Aircraft Engineering Corp.

Rottmayer, Earl, M.S. in Ae.E.; Aeronautical Engineer, The Dow Chemical Co.

Sepulveda Riveros, Luis Alfredo, B.S. in Ae.E.; 2nd Lieut., Engineering Div., Chilean Air Force.

Steiner, John Edward, M.S. in Ae.E.; Flight Engineer & Aerodynamicist, Boeing Aircraft Co.

Strausser, Charles B., Tool Design Draftsman, Goodyear Aircraft Corp.

Theriault, Paul W., B.S. in Ae.E.; Test Engineer, Wind Tunnel, Lockheed Aircraft Corp.

Warner, A. A., Aircraft Tool and Jig Designer, El Segundo Div., Douglas Aircraft Co.

Wayman, W. E., Jr., B.S. in Ae.E.; Assistant Instructor, Rensselaer Polytechnic Inst.

Wilson, Robert Slaughter, Electrical Layout Engineer, Airplane Div. (Columbus Plant), Curtiss-Wright Corp.

Wright, Howard R., Jr., B.S. in Ae.E.; Engineer, Aerodynamics Dept., Airplane Div., Curtiss-Wright Corp.

Young, P. H., Layout Draftsman, Waco Aircraft Co.

Necrology

James M. Schoonmaker, Jr.

James M. Schoonmaker, Jr., A.F.I.Ae.S., a Founder Member of the Institute, died at his home at Sewickley Heights, Pa., on December 1, 1941. He was President of General Aviation Corporation of Baltimore from 1930 to 1934. Since his retirement from aviation he had served as a Director of the Standard Steel Spring Company, the Union Spring and Manufacturing Company and the Union Storage Company of Pittsburgh.

He was graduated from Princeton University in 1911 with an electrical engineering degree and took a post-graduate course at the Massachusetts Institute of Technology.

At the time of the World War he was commissioned a Major of the United States Army Air Service, Engineering Division. He served then as chief engineer in charge of the construction of Army airplanes at the Dayton-Wright Aeroplane Company.

Mr. Schoonmaker served later as a Director of Transcontinental and Western Air, Inc., President of the General Aviation Corporation and its subsidiary, the Fokker Aircraft Corporation, which became the General Aviation Manufacturing Company, and as Vice-President and a Governor of the Aeronautical Chamber of Commerce of America.

Louis William Greve

Louis W. Greve, President and a Director of the Cleveland Pneumatic Tool Company, died on February 2, 1942, at Fort Lauderdale, Florida. He was an Associate Fellow and a Founder Member of the Institute.

Mr. Greve was born in Cleveland, Ohio, November 2, 1882, and attended public schools there. He had been associated with the Cleveland Pneumatic Tool Company since 1900. Under his direction the company designed and manufactured the first oleo shock absorbing landing gear strut for aircraft. He was also President and a Director of Champion Machine & Forging Co., Cleveland Rock Drill Co., Cleveland Pneumatic Tool Co. of Canada, Ltd., and Vice-President of the Carey Machine Co.

Mr. Greve was a founder and President of the non-profit organization of Cleveland business men which sponsored the National Air Races held at the Cleveland Municipal Airport from 1930 to 1939. He and the Cleveland Pneumatic Tool Co. sponsored the Louis W. Greve Trophy given annually at the National Air Races for speed competition of airplanes with motor displacement of 549 cubic inches or less over a 200 mile closed course.

Mr. Greve was active in financial, civic and fraternal organizations in Cleveland and was a member of the American Institute of Mining & Metallurgical Engineers, the Society of Automotive Engineers and the National Aeronautic Association.

Personnel Opportunities

The Personnel Bureau serves individual members, as well as organizations seeking to employ aeronautical specialists. Any member or organization may have requirements listed without charge.

Wanted

Experienced layout designer for permanent position with small well-established Eastern Company engaged in Government Contract Work. Address reply to Box 147, Institute of the Aeronautical Sciences.

Instructors (two) familiar with airplane design, salary $2200 a year; **Research Assistants** (two) with no teaching duties, familiar with aerodynamic research, stipend $900 plus income from research work, opportunities for graduate work; **Teaching Assistants** (three) in engine, structural and aerodynamic laboratories, stipend $900 first year, opportunities for graduate work; **Fellow** for specialized research, no teaching duties, stipend $750, opportunities for graduate work, appointment June 15th. Location east with large university. Give educational background, professional experience, photograph, in letter of application. Address reply to Box 150, Institute of the Aeronautical Sciences.

Approved Aircraft School in midwest desires mechanic and engineering instructors. Furnish qualifications, experience and snapshot in first letter. Address reply to Box 152, Institute of the Aeronautical Sciences.

Available

Aeronautical Engineer with five years' aircraft experience of which four and a half have been in the engineering department of a major aircraft company. Holds C.A.A. Ground Instructor, Private Pilot licenses and California State Department of Education teaching credentials for aeronautics. Desires position with school or university offering opportunity to teach aeronautical subjects while obtaining formal education. Address reply to Box 148, Institute of the Aeronautical Sciences.

The Technical Information Service

of the

Institute of the Aeronautical Sciences

This service has experienced personnel under the supervision of trained aeronautical engineers to compile any information desired. The services range from listing specialized reference books to the preparation of exhaustive bibliographies, digesting of reports and general surveys of any aeronautical subject. Some of the available services are:

Bibliographies on any aeronautical subject.
Reports on any aeronautical subject.
Digests of aeronautical books, papers, periodicals and references.
Translations in all languages.
Engineering investigations of special aeronautical subjects.
Biographies of individuals engaged in aeronautics.
Photostats of any aeronautical or general engineering material.
Microfilms made on special order.
Photographs made from the Institute's photographic collection.
Drawings and tracings made.

In addition to the services mentioned any commission which comes within the scope of the Service will be accepted.

Research work is charged at the usual library fee of $2.00 per hour. Special arrangements may be made for work requiring several weeks or months.

Translators are available for accurate transcriptions of all foreign language data. Translations are carefully edited by trained engineers at the standard rate of 1¢ per word. Minimum charge, $2.00.

Reproductions of any material in the Aeronautical Archives of the Institute may be ordered at standard photostat rates.